Sonja Rittchen, BSc.

Unravelling Differential Expression of Hematopoietic PGD Synthase in Macrophages and Leukocyte Subsets with Focus on Pulmonary Inflammation

MASTER'S THESIS

To achieve the university degree of

Master of Science (MSc.)

Master's degree programme: Biochemistry and Molecular Biomedical Sciences

Submitted to

Graz University of Technology

Supervisors

Univ.-Prof. Dr.med.univ. Akos Heinemann
Institute of Experimental and Clinical Pharmacology, Medical University of Graz

Univ.-Prof. Mag. Dr.rer.nat. Andreas Kungl
Institute of Pharmaceutical Sciences, University of Graz

Graz, August 2016

EIDESSTATTLICHE ERKLÄRUNG

Ich erkläre an Eides statt, dass ich die vorliegende Arbeit selbstständig verfasst, andere als die angegebenen Quellen/Hilfsmittel nicht benutzt, und die den benutzten Quellen wörtlich und inhaltlich entnommenen Stellen als solche kenntlich gemacht habe. Das in TUGRAZonline hochgeladene Textdokument ist mit der vorliegenden Masterarbeit identisch.

Graz, am …… ……..

(Unterschrift)

AFFIDAVIT

I declare that I have authored this thesis independently, that I have not used other than the declared sources/resources, and that I have explicitly indicated all material which has been quoted either literally or by content from the sources used.
The text document uploaded to TUGRAZonline is identical to the present master‘s thesis.

…… ……..

date (signature)

In cooperation with:

Medical University of Graz

Institute of Experimental and Clinical Pharmacology

Univ.-Prof. Dr.med.univ. Akos Heinemann

Acknowledgements

My first acknowledgement and biggest gratitude goes to Prof. Dr. Akos Heinemann for taking me in and enabling me to work on this great project for my Master's thesis. I deeply thank him for being my supervisor and always having an open ear for major or minor concerns, but especially for his invaluable advice and open mind for suggestions. My special thanks go to Katharina Jandl for supervising me during my Master's thesis project at the Institute. I cannot tell how thankful I am for having had the pleasure to have been introduced to everything, guided and encouraged by her throughout my project, not to mention her great support and scientific advice that never failed to motivate me. Additionally, I would like to thank Dr. Rufina Schuligoi for scientific discussions and suggestions and Prof. Kungl for taking the responsibility of being my internal supervisor at the University of Graz.

Further, I would like to thank Kathrin, Silvia and Iris for isolating leukocytes for me as well as Wolfi, Ilse and Martina for supporting me whenever I needed help. I had the privilege to work with amazing colleagues including Anna, Kathrin, Robert, Georg, Miriam and Thomas, who were always willing to share their thoughts with me and to offer advice, but most of all for making me feel welcome and appreciated right from the beginning. Additionally, I want to thank Prof. Ghaffari Tabrizi-Wizsy for offering me the opportunity to use the CAM assay and introducing me to the technique.

Many thanks go as well to my sister Ines and Theresa for their company, support and for providing me with food whenever I didn't have time to cook. Ines, I cannot tell you how much I value our conversations and the time we spend together. Also I am really grateful for my friend's support, thanks Christoph, Michelle, Denise, Anna, Stefan, Silvia and Teresa for the countless times I was allowed to spend with you. My special thanks to my Kremser grils Alex, Sigi, Lena, Nati, Laura, Sarah and Ida, who never fail to cheer me up. Not to forget, I greatly appreciate all the support and help I get from my parents, but also their concerns and advice, thank you for making everything possible.

Abstract

Prostaglandin (PG) D_2 is a potent lipid mediator with a bi-potential role in pulmonary inflammation. In the lung, circulating monocytes may infiltrate inflamed tissue, release mediators modulating inflammation or differentiate to macrophages, which in turn play a crucial role in promoting, regulating and resolving inflammatory processes. Recently, elevated PGD_2 levels were identified in a mouse model of acute lung injury with a novel strong link to macrophages as potential source of PGD_2. We hypothesize that PGD_2 production by monocytes or monocyte-derived macrophages (MDM) plays an important role in respiratory inflammatory reactions, possibly exceeding PGD_2 production by mast cells under specific pathological conditions. Indeed, we were primarily interested in the influence of macrophages in combination with PGD_2 on lung pathology. This included neovascularization in the lung, which is often dysregulated in pulmonary disorders. As activated DP1 and DP2 receptors on macrophages contribute potently to a pro-inflammatory response in the lung, we hypothesized an anti-angiogenic effect of PGD_2-stimulated macrophages.

Human monocytes were isolated from symptomatic allergic and healthy donors, and were differentiated into MDM and activated with either INF-γ/LPS (M1) or IL-4 (M2) *in vitro*. Expression of hematopoietic PGD synthase (HPGDS), the rate-limiting enzyme in PGD_2 production in peripheral tissues, was assessed on protein level by flow cytometry and Western blotting and on mRNA level by RT-qPCR. Additionally, HPGDS expression in human peripheral blood leukocytes was evaluated by flow cytometry. Furthermore, murine alveolar macrophages from ovalbumin-induced allergic airway inflammation, alveolar macrophages from lipopolysaccharide (LPS)-induced acute lung injury as well as from naïve mice were isolated. PGD_2 released by monocytes, monocyte-derived macrophages and alveolar macrophages was quantified in conditioned medium by ELISA. To assess angiogenic properties of PGD_2-stimulated macrophages, neovascularization in a chicken chorioallantoic membrane (CAM) assay was recorded.

In this study we could show that HPGDS is selectively upregulated during human macrophage differentiation *in vitro* and PGD_2 secretion is most effectively induced by priming with bacterial lipopolysaccharide in combination with interferon-gamma (INF-γ) in human monocytes and MDM. Further, alveolar macrophages isolated from a LPS-induced mouse model of acute lung injury released significantly more PGD_2 than alveolar macrophages isolated from naïve or ovalbumin-challenged mice. Circulating $CD4^+$ T-cells, NK cells, NK/T cells and plasma cells could be identified as potential PGD_2 sources by means of a flow

cytometric screening for HPGDS expression. Finally, preliminary experiments indicate that PGD_2 treatment of MDM diminishes pro-angiogenic effects in homeostatic macrophages.

Here we shed more light on the role of hematopoietic prostaglandin D synthase in human macrophages and circulating leukocytes and its potential role in inflammatory reactions in the lung. Once its role in inflammation is clear, inhibition of HPGDS poses a novel approach for modulating or preventing pro-inflammatory signalling, thereby averting tissue injury. Regarding angiogenic properties of macrophages, further investigation is needed to identify involved factors, but these findings could be exploited in the future to modulate neovascularization in pulmonary diseases.

Zusammenfassung

Prostaglandin (PG) D_2 ist ein Lipidmediator, der eine vielfältige Auswirkung auf pulmonäre entzündliche Reaktionen haben kann. Während einer Entzündung kann die Lunge von zirkulierenden Monozyten infiltriert werden, die verschiedene entzündungsfördernde oder -hemmende Faktoren sekretieren. Zusätzlich haben Monozyten das Potential sich in Makrophagen zu differenzieren, die wiederum eine zentrale Rolle in der Entzündungsförderung, -modulation und -auflösung haben. Vor kurzem wurde erhöhte PGD_2-Präsenz in einem Mausmodell von akuter Lungeninsuffizienz mit Makrophagen als potentieller Ursprung der Erhöhung in Verbindung gebracht. Unsere Hypothese inkludiert, dass PGD_2-produzierende Monozyten und von Monozyten abstammende Makrophagen eine wichtige Rolle in pulmonären Entzündungen spielen, wobei das Ausmaß an freigesetztem PGD_2 das von Mastzellen unter bestimmten Umständen übertreffen könnte. In erster Linie lag unser Fokus auf der Auswirkung von Makrophagen in Kombination mit PGD_2 auf die Lungenpathologie, was auch die Bildung von neuen Blutgefäßen, die in pulmonären Erkrankungen oft heterogen ist, mit einbezieht. Nachdem aktivierte DP1 und DP2 Rezeptoren auf Makrophagen eine starke proinflammatorische Wirkung haben, nahmen wir an, dass eine Aktivierung der Rezeptoren zugleich einen hemmenden Effekt auf die Bildung von neuen Blutgefäßen hat.

Humane Monozyten wurden von symptomatischen Allergikern oder Nichtallergikern isoliert und zu Makrophagen differenziert, die anschließend entweder mit INF-γ/LPS (M1) oder IL-4 (M2) aktiviert wurden. Expression der haematopoietischen PGD Synthase (HPGDS), des geschwindigkeitsbestimmenden Enzyms in der PGD_2 Produktion in peripherem Gewebe, wurde auf Proteinebene durch Durchfluss Zytometrie und Western blotting und auf mRNA-Ebene durch RT-qPCR evaluiert. Zusätzlich wurde HPGDS Expression in humanen Leukozyten mittels Durchfluss Zytometrie bestimmt. Alveolarmakrophagen wurden aus einem Ovalbumin-induzierten, allergischen Asthma Mausmodell, einem Mausmodell von Lipopolysaccharid-induzierter, akuter Lungeninsuffizienz und aus naïven Mäusen isoliert. PGD_2 sezerniert *in vitro* von humanen Monozyten und Makrophagen und von murinen Alveolarmakrophagen wurde mittels ELISA quantifiziert. Angiogenische Eigenschaften von PGD_2-stimulierten Makrophagen wurden auf der chorioallantoischen Membran von Hühnerembryonen ausgetestet.

Hier konnten wir zeigen, dass HPGDS während der Differenzierung von humanen Monozyten in Makrophagen hochreguliert wird, wobei bakterielles Lipopolysaccharid in

Kombination mit INF- γ die PGD_2 Produktion am effektivsten induzierte. Im Einklang mit diesen Resultaten konnten wir feststellen, dass murine Alveolarmakrophagen aus Lipopolysaccharid-induzierter akuter Lungeninsuffizienz signifikant größere Mengen an PGD_2 sezernierten als Alveolarmakrophagen aus dem allergischen Modell oder aus naïven Mäusen. Zirkulierende $CD4^+$ T-Zellen, NK Zellen, NK/T Zellen und Plasmazellen konnten anhand der Durchfluss-zytometrischen Ergebnisse für HPGDS Expression als potentielle PGD_2 Quellen identifiziert werden. Die ersten Versuche zum Thema Angiogenese weisen darauf hin, dass eine PGD_2-Stimulierung von Makrophagen einer erhöhten Bildung von neuen Blutgefäßen, die für nicht aktivierte Makrophagen sichtbar war, entgegenwirkt.

Diese Studie birgt neue Erkenntnisse sowohl über die Rolle der haematopoietischen PGD synthase in humanen Monozyten, Makrophagen und zirkulierenden Leukozyten als auch über den Einfluss von PGD_2 in verschiedenen Arten von Lungenentzündung. Sobald die Rolle von HPGDS vollkommen entschlüsselt ist, bietet sich die Möglichkeit, das Enzym selektiv zu inhibieren, um damit einen hemmenden Effekt auf entzündliche Reaktionen zu erreichen und die Gewebsschädigung zu verringern. Hinsichtlich des Effekts von PGD_2-stimulierten Makrophagen auf die Bildung von neuen Blutgefäßen werden noch weitere Studien notwendig sein, um dieses Wissen für potentielle neue Therapieansätze nutzen zu können.

List of Figures

List of Tables

Abbreviations

Ab	antibody
AF	Alexa fluor (fluorophore)
CAM	chorioallantoic membrane
CD	cluster of differentiation
COX	cyclooxygenase
Cy	cyanine (fluorophore)
DP	D-type prostanoid receptor
ELISA	enzyme-linked immunosorbant assay
FBS	fetal bovine serum
GAPDH	glyceraldehyde dehydrogenase
GPCR	G-protein coupled receptor
HPGDS	hematopoietic prostaglandin D synthetase
HSC	hematopoietic stem cell
IC	isotype control
Ig	immunoglobin
IL	interleukin
INF	interferon
LPS	lipopolysaccharide
LPGDS	lipocalin-type prostaglandin D synthase
MAPK	mitogen-activated protein kinase
M-CSF	macrophage-colony stimulating factor
MDM	monocyte-derived macrophage
Mio	million
MOX	methoxylamine oxide
NK cells	natural killer cells
P/S	penicillin/streptomycin
PBMC	peripheral blood mononuclear cells
PBS	phosphate-buffered saline
PI3K	phostphatidyl inositol 3 kinase
PE	phycoerythrin (fluorophore)
PerCP	peridinin chlorophyll protein (fluorophore)
PG	prostaglandin
PMNL	polymorphonuclear leucocytes
PVDF	Polyvinylidene diflouride
qRT-PCR	quantitative reverse transcription polymerase chain reaction
rh	recombinant human
ROS	reactive oxygen species
RPMI	Roswell Park Memorial Institute medium
RT	room temperature
SEM	standard error of the mean
TNF	tumor necrosis factor

Table of Contents

1 Introduction

Inflammation is a multi-cellular reaction crucial for the body's defence against pathogens and potentially harmful particles. Progression or resolution of inflammatory processes highly relies on a balance between pro- and anti-inflammatory signalling between involved cells. Acute and chronic pulmonary inflammation are still extensively studied to-date as a thorough knowledge of molecular and cellular interactions is necessary for developing novel treatments for patients suffering from Acute Respiratory Distress Syndrome (ARDS), Chronic Obstructive Pulmonary Disease (COPD) or allergic asthma. Macrophages may originate from circulating monocytes and play a key role in modulating the immune response in the lung as they are responsible for the first-line defence by phagocytosis of microorganisms and harmful particles. On the other hand, they actively participate in inflammatory reactions by releasing pro- or anti-inflammatory mediators and interact with cells responsible for the adaptive immune response [1]. Prostaglandin (PG) D_2 is a potent lipid mediator involved in various functions in the immune response and elevated levels have been found in pulmonary inflammatory disorders [2,3]. Under which conditions and to which extent monocytes, macrophages or other immune cells produce PGD_2 still needs to be deciphered.

1.1 Macrophages and monocytes in health and disease

Monocytes and macrophages are important effector cells of the immune system. They do not only play a crucial role in phagocytosis of microorganisms and dead cells but also actively participate in the immune response by releasing pro- and anti-inflammatory mediators. In the lung, macrophages play a key role in first-line defence against pathogens, link the innate and adaptive immune response and orchestrate immune cells [1].

1.1.1 The mononuclear phagocyte system

Monocytes and macrophages as well as dendritic cells belong to a network of cells that has been termed the mononuclear phagocyte system (MPS). They play a vital role in immunity and inflammatory reactions by phagocytosis, recognition of intruding microorganisms or other hazards and mediating the inflammatory process [4,5]. In adults, monocytes originate from hematopoietic stem cells that further differentiate in the bone marrow involving further committed progenitors. Fully differentiated monocytes are released into the bloodstream where they circulate, patrolling the vasculature for several days. The monocyte population can be divided into three subsets including classical human monocytes with high CD14 but no CD16 expression, an intermediate type with CD14 and CD16 expression and a non-

classical subset with low CD14 but high CD16 expression [6]. Peripheral blood monocytes are not only precursors of macrophages and dendritic cells but foremost they are potent effectors of the inflammatory response being able to perform phagocytosis, produce reactive oxygen species (ROS), nitric oxide (NO) and inflammatory cytokines [7]. They may also be involved in angiogenesis and arteriogenesis under certain circumstances [8].

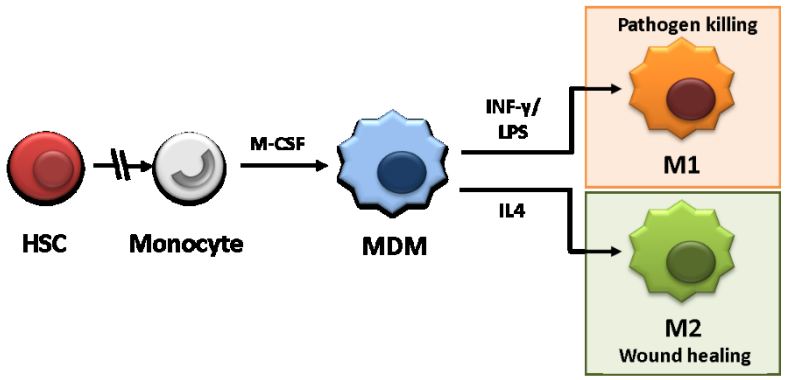

Figure 1. Origin of monocyte-derived macrophages (MDM). Peripheral blood monocytes originate from hematopoietic stem cells in the bone marrow. Upon stimulation with M-CSF monocytes differentiate into monocyte-derived macrophages. MDM can be further activated to M1 or M2 macrophages.

A monocyte-macrophage dendritic cell progenitor (MDP) has been identified, confirming that monocytes may differentiate into both - macrophages and dendritic cells - upon stimulation with M-CSF or GM-CSF, respectively [9]. Historically, there was a strict classification of mononuclear phagocytes by cell surface markers and specific function e.g. phagocytosis for macrophages; however, ongoing research identifies more and more combinations of functions with surface markers which hampers a discrete differentiation between cell types [10]. Nevertheless, it has proven certainly useful to define two opposing phenotypes of activated macrophages when looking at pro- or anti-inflammatory stimuli. Guilliams & van de Laar refer to this model as ‘discrete polarization model’ whereby stimulation of monocyte-derived macrophages with INF-γ and bacterial endotoxins like LPS generates a pro-inflammatory, pathogen killing phenotype (M1 macrophages) while stimulation with IL-4, IL-10 or IL-13 induces a wound healing, tissue remodelling phenotype (M2 macrophages).

1.1.2 Origin and function of tissue macrophages in the lung

Macrophages are distributed throughout the body and play a crucial role in maintaining tissue homeostasis, linking innate and adaptive immune response and modulating inflammation. In the lung, at least three types of resident macrophages can be found including interstitial, bronchial and alveolar macrophages that are exposed continuously to various kinds of particles, toxins, allergens and infectious agents [11]. Thus, these cells are key players in modulating an immune response against possibly harmful intruders. For a long time it was considered that all tissue macrophages originate from circulating monocytes, therefore, being descendants of bone marrow hematopoietic stem cells [12]. However, it has been shown recently that most adult tissue macrophages originate from embryonic cells rather than from circulating monocytes [13]. In early embryonic development, yolk-sac-derived macrophages can be observed and, to a later stage, macrophages derived from definitive hematopoietic stem cells in the embryonic liver.

In mice, alveolar macrophages develop from fetal monocytes that populate alveoli shortly after birth and become self-maintaining throughout life [14]. Residing in alveoli, they are highly exposed and act as first-line defence as the predominant phagocytic cells in the alveolar space. Besides alveolar macrophages, which comprise the majority of resident macrophages in the lung, interstitial macrophages are found that have been linked to antigen presentation and a lower phagocytic activity [15]. Interstitial macrophages have been proposed to be the intermediate between monocytes and alveolar macrophages; also higher turnover rates in comparison to alveolar macrophages suggest a continuous replacement of interstitial macrophages by circulating monocytes [16]. In the healthy lung the majority of alveolar macrophages are derived from embryonic progenitors, which are also able to proliferate and repopulate alveoli after depletion. However, if there is a genotoxic injury of resident macrophages or an ongoing inflammation, blood monocytes migrate across the vascular barrier, differentiate into monocyte-derived macrophages and outcompete resident macrophages [13]. This suggests a complex and crucial role of macrophage heterogeneity in health and disease, and emphasizes the need of a well-balanced state between resident and monocyte-derived macrophages in the lung.

1.1.3 Classically and alternatively activated macrophages

As mentioned earlier, macrophages show highly heterogeneous characteristics but it has proven practical to group them to either a pro-inflammatory or an anti-inflammatory phenotype. Depending on the microenvironment in which macrophages are found in, they

are exposed to various activation factors, generating multiple subsets tremendously differing in cytokine production and function [17].

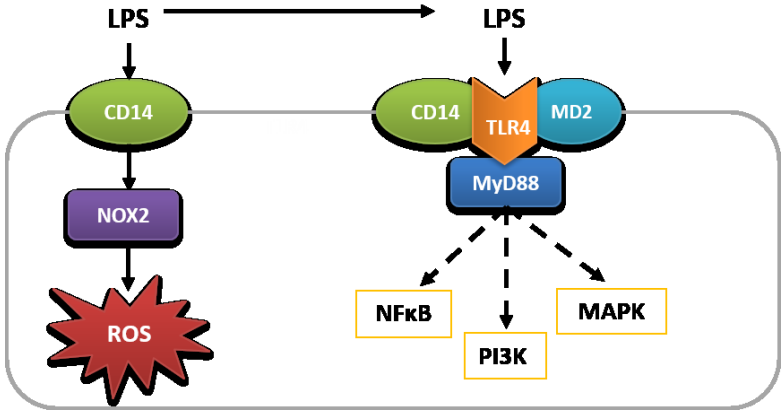

Figure 2. LPS activates the TLR4 receptor complex and downstream signalling. LPS is recognized by CD14, which activates NOX-2 and results in ROS production. LPS-bound CD14 associates with TLR4 and MD2, thereby activating MyD88 and downstream signalling targets.

Classically activated macrophages are referred to as M1 macrophages with a pro-inflammatory phenotype and are involved in the first response of pathogen killing. They are associated with a high ROS production, expression of inducible nitric oxide synthase (iNOS) and enhanced secretion of inflammatory cytokines including IL-1, IL-6 and tumor necrosis factor (TNF)-α [18]. Macrophages can be primed by INF-γ secreted by Th1 cells and activated with TNF, or an inducer of TNF such as lipopolysaccharide. LPS is a bacterial endotoxin originating from gram-negative bacteria which activates Toll-like receptor 4 (TLR4) downstream signalling, thereby inducing also NADPH oxidase (NOX) 2, that is needed for ROS production [18]. CD14, another pattern recognition receptor, and LPS-binding protein (LBP) recognize LPS and act as co-receptor for the TLR4/MD-2 heterodimer (Fig.2) [19]. Downstream signalling events are triggered, including activation of nuclear factor κB (NFκB), phosphatidyl inositol 3-kinase (PI3K) and activation of the mitogen-activated protein kinase (MAPK) pathway resulting in upregulation of pro-inflammatory cytokines and products needed for ROS production. M1 macrophages are identified by up-regulation of surface molecules including MHC class II and B-7 (CD86/CD80) [18,20].

Alternatively activated macrophages associated with wound healing and tissue remodelling are referred to as M2 macrophages. The cytokines IL-4 and IL-13 are released in Th2-type inflammation, which is typical for allergic reactions or immune responses against parasitic and extracellular pathogens [21]. Here, we focus on IL-4 activated M2 macrophages that are

mostly involved in wound healing and tissue remodelling. IL-4 as well as IL-13 is recognized by IL-4 receptor α (IL-4Rα) thereby activating the phosphorylation of signal transducer and activator of transcription (STAT) 6 and adenosine monophosphate-activated kinase (AMPK) resulting in the upregulation of M2-like features, including secretion of arginase 1, TGF-β, IL-10 and mannose receptor (CD206) expression [21,22]. Arginase 1 is an enzyme needed for extracellular matrix production and remodelling while IL-10 and TGF-β have anti-inflammatory effects. Additionally, arginase counteracts INF-γ-induced upregulation of iNOS resulting in impaired ROS production by M2 macrophages [21]. However, if IL-4-primed macrophages are exposed to triggers of classical activation (e.g. INF-γ and LPS) this causes a phenotype switch and potentiation of pro-inflammatory effects [23]. Besides having the potential to resolve inflammation, high numbers of alternatively activated macrophages are present in lungs of COPD patients and this has been related to driving disease progression; while the underlying mechanisms are not completely evaluated to-date, production of IL-13 and chitinase 1 by M2 macrophages seems to be involved [24].

1.1.4 Macrophage polarization and its influence on angiogenesis

Besides playing a key role in modulating inflammatory reactions, macrophages have also been shown to be involved in regulating angiogenesis. A strict balance of pro- and anti-angiogenic factors is responsible for blood vessel homeostasis. A dysregulation in angiogenesis is a crucial feature in many diseases including cancer and pulmonary fibrosis [25,26]. Classically activated macrophages release pro-inflammatory factors and at the same time have been linked to anti-angiogenic properties, while alternative activation of macrophages results in the opposite [27]. In cancer, the majority of tumor-associated macrophages are alternatively activated by IL-4, IL-10 or IL-13. M2 macrophages release angiogenic factors including vascular endothelial growth factor (VEGF) as well as pro-angiogenic cytokines like IL-23 and IL-17 [25]. On the other hand, chronic inflammation has been associated with tumor onset and involves elevated levels of TNF-α, which may be released by classically activated M1 macrophages, thereby also promoting tumor growth and angiogenesis [28].

1.2 Leukocyte subsets involved in inflammation

Recruitment of immune cells from peripheral blood into sites of inflammation is a key feature of tissue damage or infection. Besides macrophages, which play a crucial role in orchestrating the inflammatory response, the first-line response also involves other cells of the innate immune system including granulocytes, which goes along with activation of lymphocytes, cytokine production and progression of inflammation. Progression or resolution of inflammation is highly dependent on the presence of differentially activated leukocytes in affected tissues.

1.2.1 Granulocytes

Peripheral blood granulocytes include neutrophils, eosinophils and basophils, which are important mediators of the inflammatory response and typically contain granules with effector molecules characteristic for each type. They are recruited from the blood into inflamed tissue by cell-specific chemokines where they participate in defence reactions. Eosinophils play an important role in protection against parasites e.g. helminth infection but also in sparking the inflammatory response in allergy and bronchial asthma [29,30]. Degranulation of eosinophils results in the release of cytotoxic and pro-inflammatory mediators including IL-4, IL-5, IL-10 and IL-13 [31].

Neutrophils as well as eosinophils belong to the polymorphonuclear leukocytes (PMNL) which have a characteristically lobed nucleus. Being able to phagocytose harmful intruders and cell debris, neutrophils play an important role in the first immune response [32]. Additionally, they are able to promote inflammation by degranulation and activate various inflammatory mechanisms with the content of their granules; therefore, their action needs to be controlled tightly to avoid excessive tissue damage.

1.2.2 Lymphocytes

Besides first-line defence by cells of the innate immune system, B- and T-lymphocytes are the major key players of the adaptive response in inflammation. They interact with antigen-presenting cells including macrophages and dendritic cells and initiate the humoral immune reaction against intruders. The lymphocyte population also includes NK cells, which are mainly responsible for cytotoxic reactions.

T-cells originate from bone marrow-derived progenitor cells, while maturation progresses in the thymus where they develop a specific T-cell receptor (TCR). CD3 is typically expressed

by T-cells as it acts as co-receptor for the TCR complex [33]. Additionally, mature T-lymphocytes express either CD4 or CD8 as TCR co-receptor, whereby the first allows interaction with major histocompatibility complex (MHC) II and the latter with MHC I [34]. $CD8^+$ T-cells are cytotoxic cells that are activated by recognizing a MHC I -bound antigen (e.g. virus) and release perforin and granzymes upon binding this specific complex, thereby inducing cytolysis of the infected cell. $CD4^+$ T-cells are involved in defence against foreign intruders like microbes by interacting with antigen-presenting cells and are referred to as helper T (Th) cells, which can be further divided into different subsets according to cytokine profiles. Th1 cells release pro-inflammatory cytokines including INF-γ and TNF-α which play an important role in neutrophilic type-1 inflammation [35]. Th2 cells produce IL-4, IL-5 and IL-13 and help in facilitating antibody production by B-cells. IL-4 and IL-5 enable IgE production by B-cells and IL-5 also is a strong differentiation factor for eosinophils and promotes their locomotion; thus, Th2 cells play an important role in allergic type-2 reactions [34,36].

In addition, there are NK cells with no antigen-specific receptors and NK/T cells, which express antigen-specific receptors typical for T lymphocytes, both of which are involved in cytotoxic reactions [37].

B-lymphocytes facilitate humoral immunity by their ability to produce antigen-specific antibodies that neutralize pathogens and toxins, facilitate opsonisation and activate the complement system. They originate from and mature in the bone marrow from where they are released into circulation. After maturation in the bone marrow and final stages of development in the spleen, mature B cells circulate mostly in the lymphatic system until they encounter an antigen that specifically binds their B-cell receptor or they undergo cell death [38]. Naïve B-cells are activated in lymphoid tissues by B-cell receptor cross-linking with antigen-presenting cells and T-cell facilitate the interaction [34]. Activation through specific antigen-B-cell receptor binding triggers rapid proliferation of B cells and differentiation into plasma cells (effector B cells) or memory B cells. Plasma cells are not-dividing effector cells that are able to produce and secrete great amounts of antibodies [39]. Additionally, there is evidence that effector B-cells (plasma cells) contribute to cytokine production, thereby, actively influencing regulation of immunity [38].

1.3 Pulmonary inflammation

Respiratory diseases like pneumonia and allergic asthma have remained the top major killers during the past decade right after ischemic heart disease and stroke according to the WHO (2014). Although onset and disease progression differ between the major classes of

pulmonary inflammation including acute respiratory distress syndrome (ARDS) and allergic asthma there are certain similarities. Inflammation is a highly dynamic process leading to a specific lung pathology; however, common symptoms of pulmonary inflammation include airway insult and restriction of gas exchange causing shortness of breath and coughing [40].

1.3.1 Acute respiratory distress syndrome (ARDS)

Acute respiratory distress syndrome (ARDS) is associated with multiple risk factors that trigger respiratory failure. A less severe form is referred to as acute lung injury (ALI) resulting in critical respiratory impairment, but shows a slightly lower level of hypoxia [41]. With sepsis and pneumonia being the leading causes of ARDS there is a mortality of 30 – 50 % in affected patients. Common characteristics of ARDS-related pulmonary insufficiency include hypoxia, as well as increased permeability resulting in alveolar edema and neutrophil infiltration [42,43]. Changes in pulmonary permeability may occur as a direct response to bacterial endotoxins like lipopolysaccharide, thus, facilitating neutrophil infiltration into the injured tissue. Neutrophils produce pro-inflammatory cytokines such as TNF-α, IL-1β and contribute thereby to further inflammation [44]. Alveolar macrophages orchestrate neutrophil recruitment in ALI and play a crucial role in disease development [45]. Mechanic ventilation is still used as standard therapy of ARDS despite tremendous research efforts since ARDS was first characterized in 1967. Recently, it has been shown that activated PGD_2 receptors on macrophages have a pro-inflammatory effect which poses a potential new pharmacological target to alter disease progression [46]. A novel therapeutic approach is to regulate alveolar macrophage response in ALI, thus preventing neutrophilic infiltration, and reducing inflammation.

1.3.2 Allergic airway inflammation and asthma

Asthma is a result of airway hyper-responsiveness causing acute and chronic inflammation, mucus secretion and tissue remodelling. It is, however, a highly heterogeneous disorder including various phenotypes differing in severity and cellular composition involved in inflammation, e.g. eosinophilic asthma or neutrophilic asthma. Onset is predominantly triggered by an allergic reaction dominated by Th2-type lymphocytes followed by an ongoing irritation in the airways upon exposure to the antigen [47]. Patients suffer from shortness of breath and coughing caused by airway swelling. They may need hospitalization to prevent hyperventilation and suffocation. Repeated cycles of inflammation are typical for asthma, causing lung injury followed by long-term structural changes of the airways termed ‘remodelling’. At this point, there is still no cure for asthma, which makes long-term treatment necessary to control symptoms. Most common prescriptions are

avoidance of environmental allergens triggering a reaction, beta-adrenergic bronchodilators and corticosteroid inhalation [48].

The inflammatory response involves eosinophils, neutrophils, dendritic cells, macrophages, $CD4^+$ T-lymphocytes and mast cells. Still, eosinophil infiltration is highly characteristic for asthmatic inflammation [49,50]. Allergy-associated asthma, the most common form, is triggered by an IgE-dependent reaction to an allergen mediated by T-lymphocytes. This results in mast cell activation which in turn initiates pro-inflammatory cytokine release by mast cells and eosinophils [51]. Upon mast cell degranulation, histamine is released, which further provokes inflammation and along with histamine, PGD_2 is released at approximately same concentrations acting on immune cells expressing PGD_2 receptors including eosinophils, T-cells and macrophages [52]. However, to which extent macrophages are involved in asthma and allergic inflammation in the lung still needs to be elaborated.

1.3.3 Selected mouse models of pulmonary inflammation

Ovalbumin (OVA) challenge-induced mouse model of allergic asthma

The OVA-challenge model is the most commonly used method to induce allergic pulmonary inflammation. It includes a sensitisation phase (14 – 21 days) in which the allergen (OVA) is systemically administered along with an adjuvant such as aluminium hydroxide ($Al(OH)_3$) that promotes the development of a Th2-type inflammatory reaction. Following sensitisation, mice are challenged with OVA through the airways by inhalation, intranasal or intratracheal, over a period of time [53]. This model allows primarily investigating disease processes in allergic asthma including cellular and molecular mechanisms of inflammation, but it is not suitable for long-term studies as the sensitisation is only temporary.

Lipopolysaccharide (LPS) – induced mouse model of acute lung injury (ALI)

Bacterial endotoxins like LPS are potent activators of inflammation as their presence indicates invasion of potentially harmful microorganisms. LPS exposure causes acute lung injury of which typical hallmarks include acute injury to epithelial and endothelial barriers in the lung, leukocyte, mostly neutrophil, infiltration and pulmonary edema. Inflammatory effects are mostly due to activation of TLR4 on monocytes and macrophages thereby inducing ROS production and pro-inflammatory signalling. This model closely resembles ALI/ARDS in humans and facilitates uncovering cellular mechanisms and interactions as well as elucidating potential new treatments to diminish over-the-top inflammatory reactions [54].

1.4 Prostaglandin D_2 – origins and physiological effects

1.4.1 The cyclooxygenase pathway and generation of PGD_2

PGD_2 is a lipid mediator with a wide range of physiological effects on inflammatory reactions, pain and fever amongst others. Prostaglandins as well as prostacyclins (PGI), thromboxanes (TX), leukotrienes (LT) and lipoxins (LX) belong to the eicosanoids, which are a group of molecules derived from the C_{20} fatty acid, arachidonic acid. PG, PC and TX in turn are referred to as prostanoids which are synthesised by the cyclic pathway [55]. Eicosanoids are potent mediators, which act locally through auto- or paracrine effects by binding relevant G-protein coupled receptors (GPCR). The first step in PGD_2 synthesis (Figure 3) is the release of membrane phospholipid-derived arachidonic acid by phospholipase A_2 (PLA_2). Cytosolic PLA_2 can be activated by enhanced serine phosphorylation of the enzyme induced by stimulants including zymosan, Ca^{2+}-ionophores but may also be hormone-mediated through e.g. epinephrine [56]. Arachidonic acid is a substrate for constitutively expressed cyclooxygenase (COX)-1 as well as COX-2, which is upregulated by pro-inflammatory stimuli [57]. Both COX enzymes have a dual function with cyclooxygenase and peroxidase activity, thus, being able to catalyse the isomerization of free arachidonic acid to PGH_2 with PGG_2 as intermediate. PGH_2 further acts as starting point for the production of prostanoids by corresponding synthases including PGE_2, PGD_2, TXA_2, TXB_2 and PGI_2. Depending on the cell type and microenvironment, cells may change their prostanoid production profile. A change in intracellular balance between prostanoids, e.g. the ratio between PGE_2 and PGD_2, is a crucial indication in the development of many diseases including bronchial asthma [58]. PGD_2 is produced by isomerization of PGH_2 which is catalysed by either hematopoietic prostaglandin D synthase (HPGDS) or lipocalin-type prostaglandin D synthase (LPGDS), two vastly different

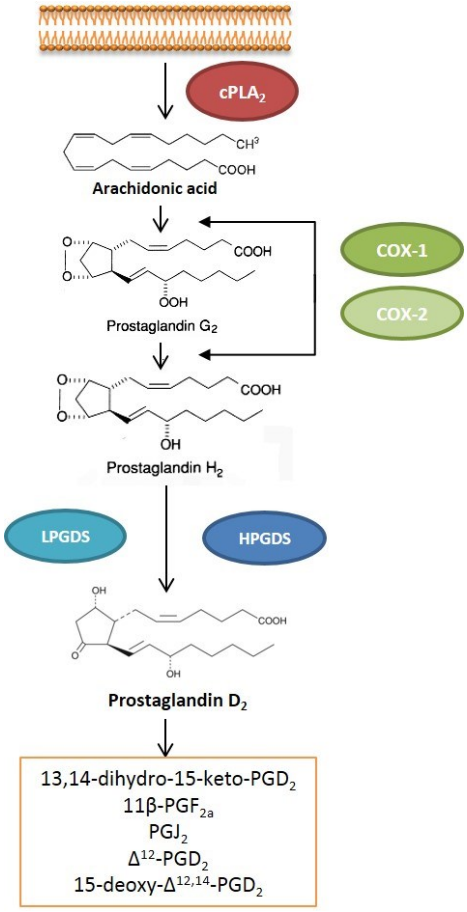

Figure 3. PGD_2 generation from arachidonic acid. Arachidonic acid is released from phospholipid membranes by cytosolic PLA_2, which is converted by COX to PGH_2. PGH_2 conversion into PGD_2 is catalyzed by HPGDS or LPGDS. PGD_2 can be further metabolized to bioactive compounds.

enzymes catalysing the same reaction [59]. Furthermore, as PGD_2 has a short half-life, about 30 minutes in plasma, and is rapidly metabolized thereby forming several bioactive degradation products including 13,14-dihydro-15-keto-PGD_2, 11β-PGF_{2a}, PGJ_2, Δ^{12}-PGD_2 and 15-deoxy-$\Delta^{12,14}$-PGD_2 [60].

1.4.2 Distribution and function of Prostaglandin D synthases

There are two distinct types of rate-limiting PGD synthases, one termed lipocalin-type PGD synthase (LPGDS) and the other hematopoietic PGD synthase (HPGDS), which differ vastly in origin, structure, tissue distribution, cellular localization and functional relevance [59].

The hematopoietic prostaglandin D synthase is a Sigma-class glutathione transferase and catalyses the isomerization of PGH_2 to PGD_2 using reduced glutathione (GSH) and Ca^{2+} or Mg^{2+} as cofactor. Zhao et. al. could show that reactive oxygen species (ROS) are crucial for proper HPGDS function [61]. Additionally, there is evidence that HPGDS activity is dependent on pH which has an impact on H^+ abstraction from the GSH thiol group [62]. The enzyme forms a homodimer with 23 kDa subunits each one associated with one GSH and X-ray crystallography revealed a compact structure containing α-helical and β-sheet structures [63].

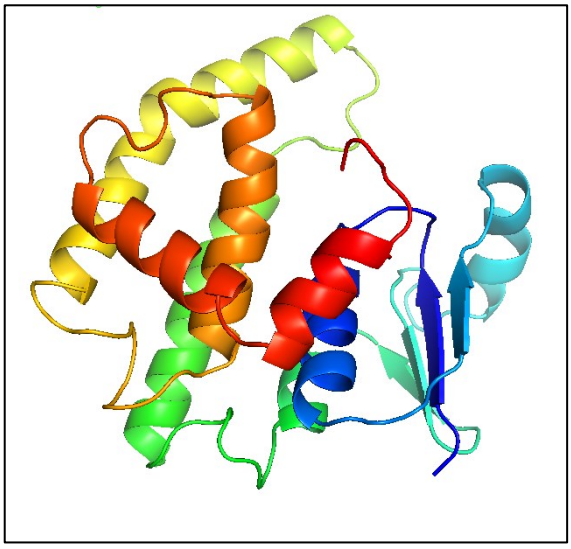

Figure 4. Crystallographic structure of a human HPGDS-monomer modelled with Phyre2 [95].

Site-directed mutagenesis experiments indicate that Lys112, Cys156, and Lys198 are involved in the binding of PGH_2, Trp104 is critical for structural integrity of the catalytic centre for GST and PGDS activities, and Tyr8 and Arg14 are essential for activation of the thiol group of glutathione [64]. HPGDS is expressed in peripheral tissues and it has been localized in antigen-presenting cells, mast cells, megakaryocytes and Th2 lymphocytes; whereby, PGD_2 production by mast cells was characterized thoroughly in comparison to other eventual sources, thus, linking HPGDS functional activity primarily to pro-inflammatory and anti-angiogenic stimulation [65–67]. However, hematopoietic PGD synthase has also been shown to be crucial for suppressing bleomycin-induced lung injury [68].

In contrast, LPGDS is primarily localized in the central nervous system, reproductive tracts and also secreted into cerebrospinal fluid and the bloodstream [59]. The highly glycosylated

protein belongs to the lipocalin (lipophilic ligand-carrier protein) gene family and requires free sulfhydryl compounds for catalysing the conversion of PGH_2 to PGD_2 but not necessarily GSH. There are indications that LPGDS is involved in regulating sleep-awake phases in the brain as well as certain renal and heart malfunctions [69].

1.4.3 PGD_2 signalling via G protein-coupled receptors (GPCR)

The first G-protein coupled PGD_2 receptor to be discovered was D-type prostanoid receptor 1 (DP1 or DP). PGD_2 or PGD_2 metabolites, including Δ^{12}-PGD_2 and PGJ_2, binding to DP1 activates the $G_{\alpha,s}$ subunit, which in turn activates adenylyl cyclase (AC) resulting in elevated cyclic adenosine monophosphate (cAMP) levels and activation of cAMP-dependent enzymes including protein kinase A (PKA) [70]. Activation of DP1 downstream signalling has been linked to both pro- and anti-inflammatory effects. DP-mediated responses include inhibition of platelet aggregation, induction of vasorelaxation and bronchodilatation [71] but on the other hand, the introduction of a DP antagonist was able to prevent rhinitis, conjunctivitis and pulmonary inflammation [72] and DP1 receptor activation increased neutrophil infiltration in acute lung injury [46].

More recently, a second G protein-coupled PGD_2 receptor termed DP2 was identified, originally named chemoattractant receptor-homologous molecule expressed on Th2 cells (CRTH2). Receptor activation triggers $G_{\alpha,i}$ subunit activation, which in turn inhibits adenylyl cyclase thereby decreasing intracellular cAMP levels and increasing Ca^{2+} [73]. The $G_{\beta\gamma}$ subunit activates phospholipase C_β which generates diacylglycerol (DAG) and inositol triphosphate (IP_3) resulting in elevated Ca^{2+} levels [74]. Further, $G_{\alpha,q}$ coupling to DP2 may activate phosphatidyl inositol 3 kinase (PI_3K) and MAP kinase pathway [75]. DP2 has been associated with many pro-inflammatory effects of PGD_2 including stimulation of immune cell migration, respiratory burst of eosinophils as well as triggering histamine and cytokine release [76]. The potential of DP1/DP2 heterodimer formation and its effect on inflammatory responses still needs further investigation.

1.4.4 Pro- and anti-inflammatory properties of PGD_2

In part due to the opposing effects of DP receptors but also due to multiple sources and microenvironments in which PGD_2 is present, both pro- and anti-inflammatory effects have been related to elevated PGD_2 levels. PGD_2 is associated with homeostatic functions mostly in brain and with negative effects in airways where mast cells are involved [77].

In Igε-mediated autoimmune diseases like allergic asthma, high levels of PGD_2 are released by activated mast cells causing bronchoconstriction but also driving inflammation

and tissue remodelling [78]. Additionally, mice overexpressing LPGDS have elevated PGD_2 levels and an increased allergic response in a OVA-induced asthma model [3]. PGD_2 acts as chemoattractant for eosinophils, Th2 cells, basophils as well as neutrophils, thereby, promoting leukocyte infiltration into the lung in Th1 and Th2-type inflammatory reactions [46,73].

In contrast to these pro-inflammatory effects, PGD_2 has also been linked to mediating and resolving inflammation. Murata et. al. could show that DP agonism directly enhanced endothelial barrier function and in a later phase attenuated neutrophil infiltration in acute lung injury [79] while Ando et. al. could show that administration of HPGDS-expressing fibroblasts could alleviate bleomycin-induced lung injury [68].

The physiological effect of PGD_2 is not only dependent on elevated levels, even more interesting are how activation of the two DP receptors influences the response. Various observations indicate an anti-inflammatory effect mediated by activated DP1 receptor in the early phase of skin inflammation, however, a pro-inflammatory effect of activated DP2 receptors was found in the late phase [80].

1.4.5 PGD_2 in angiogenesis

It remains mostly speculative whether and how PGD_2 is involved in regulating angiogenesis under normal conditions or in cancer. However, in the lung PGD_2 has mostly been linked with pro-inflammatory effects, which often goes along with anti-angiogenic properties. HPGDS deficiency in mice results in enhanced progression of lung carcinoma due to increased angiogenesis while activation of DP1 receptor resulted in suppression of angiogenesis [65,67]. These findings suggest that PGD_2 reduces angiogenesis and tumor progression, however, further investigation will be needed to confirm and fully characterize PGD_2 involvement in angiogenesis.

2 Aim of this study

Elevated PGD_2 levels have been linked to various pathological features of pulmonary inflammation mostly due to promoting leukocyte infiltration and disease progression [2,81]. In allergic asthma, PGD_2 is primarily released by mast cells after IgE-receptor crosslinking, however, macrophages and other immune cells have also been considered as potential PGD_2 sources under inflammatory conditions. In peripheral tissues and cells of the hematopoietic lineage, the hematopoietic PGD synthase (HPGDS) is the rate-limiting enzyme catalysing the conversion of PGH_2 to PGD_2, which makes it an interesting target to screen for potential PGD_2 sources. Next to elevated PGD_2 levels, an increase in the number of HPGDS-positive cells, which were morphologically identified as macrophages, could be observed in lung histological sections of ARDS patients [46]. This indicates a critical role of PGD_2 and corresponding receptors, DP1 and DP2, in relation with macrophages in modulating inflammatory responses in the lung, which is in need of further investigation.

Here, we want to i) elucidate the involvement of macrophages and monocytes with regard to elevated PGD_2 levels in acute lung injury and other respiratory inflammatory processes, ii) quantify hematopoietic PGD synthase (HPGDS) expression in subsets of leukocytes and iii) investigate the influence of PGD_2 - activated macrophages on neovascularization.

3 Material and Methods

3.1 Materials

Equipment

Axiocert 40 CFL microscope	Carl Zeiss Microscopy GmbH
BCA assay kit	Thermo Scientific
CellBind surface culture plates	Corning
CFX Connect Real-Time PCR Detection System	BioRad
ChemiDoc Touch System	BioRad
ELx50 microplate washer	BioTek
FACS Canto II	BD Biosciences
PGD_2-MOX ELISA Kit	Caymen chemical
PVDF membrane (0.2 µm)	BioRad
Multi-wavelength plate reader	BioRad
Miltenyi Monocyte isolation kit II	Miltenyi

Reagents

Accutase	Sigma-Aldrich
CellFix	BD Immunocytometry Systems
Dako Antibody Diluent	Dako
FACSFlow	BD Immunocytometry Systems
FcX-receptor Block	BioLegend
Fixation/Permeabilization Kit	BD Biosciences
Fresenius double-distilled water	Fresenius
HEPES Buffer Solution 1M	PAN Biotechnology
Histopaque-1077	Sigma-Aldrich
iScript cDNA Synthesis Kit	BioRad
PGD_2	Cayman Chemicals Ann Arbor
Phosphate buffered saline (PBS) with or w/o Ca2+ and Mg2+	PAN Biotechnology
Rat-tail collagen type I	Corning
SsoAdvanced Universal SYBR Green Supermix	BioRad
UV Block	Thermo Scientific
TriReagent	Sigma-Aldrich

Antibodies

	Company	**Cat.#**
Alexa-Fluor 488 rabbit anti-mouse	Invitrogen	A11059
APC mouse anti-human CD123	BD Bioscience	560087

Horseradish peroxidase goat anti-mouse	Thermo Scientific	32430
Horseradish peroxidase goat anti-rabbit	Cell Signaling Technology	7074
Mouse anti-human HPGDS (IgG1)	Novus Bioscience	MAB6487
Mouse IgG1 isotype control	Novus Bioscience	MAB002
PE Isotype Control IgG1 kappa	BD Bioscience	559320
PE mouse anti-human CD138	BD Bioscience	561704
PE mouse anti-human CD206	BD Bioscience	555954
PE mouse anti-human CD4	BD Pharmingen	561843
PE mouse anti-human CD8	BD Pharmingen	560949
PE mouse anti-human CD80	BD Bioscience	557227
PE mouse anti-human HLA/DR	BD Bioscience	556653
PE-Cy5 mouse anti-human CD16	BioLedgend	302010
PE-Cy5.5 mouse anti-human CD3	BD Bioscience	555334
PE-Cy7 mouse anti-human CD20	BD Pharmingen	560735
PE-Cy7 mouse anti-human CD56	BD Pharmingen	560916
PerCP mouse anti-human CD14	BD Bioscience	2240746
Rabbit anti-human GAPDH	Cell Signaling	14C10
V450 mouse anti-human CD19	BD Horizon	560354

Buffer and media preparations

	Ingredients	**Company**
Cell wash buffer (pH 7.4)	PBS with Ca^{2+} and Mg^{2+}	PAN Biotechnology
	90 mM glucose-monohydrate	MERCK KGaA
	0.008 mM bovine serum albumin	Sigma Aldrich
	10 mM HEPES	PAN Biotechnology
Fixative solution (CellFix)	2.5 % CellFix	BD Immunocytometry Systems
	75 % FACSFlow	BD Immunocytometry Systems
	22.5 % Fresenius water	Fresenius Medical Care
Adhesion medium for monocytes	RPMI 1640 with stable glutamine	PAN Biotechnology
	1x P/S (100 x)	PAN Biotechnology
	1x non essential aminoacids	GIBCO Life Technologies
	1 % sodium pyruvate	Sigma Aldrich
	5 mM HEPES Buffer Solution	PAN Biotechnology
	5 % human AB serum	Sigma Aldrich
Differentiation medium for MDM	RPMI 1640 with stable glutamine	PAN Biotechnology
	1x P/S (100 x)	PAN Biotechnology
	10 % FBS	GIBCO Life Technologies

	100 ng/ml rh M-CSF	PeproTech
Polarization medium for human M1 macrophages	RPMI 1640 with stable glutamine	PAN Biotechnology
	1x P/S (100x)	PAN Biotechnology
	10 % FBS	GIBCO Life Technologies
	100 ng/ml LPS (E.coli)	Sigma Aldrich
	20 ng/ml rh INF-y	Immunotools
Polarization medium for human M2 macrophages	RPMI 1640 with stable glutamine	PAN Biotechnology
	1x P/S	PAN Biotechnology
	10% FBS	GIBCO Life Technologies
	20 ng/ml rh IL-4	Immunotools
6x western blot sample buffer	375 mM TRIS/HCl ph 6.8	Carl Roth GmbH
	12% SDS	Carl Roth GmbH
	50 % Glycerol	Sigma Aldrich
	0.003 % bromophenol blue	Sigma Aldrich
	15 % 2-mercaptoethanol	Sigma Aldrich
SDS PAGE run buffer 10x (pH 8.9)	30.3 g/l TRIS	Carl Roth GmbH
	150.1 g/l glycine	Carl Roth GmbH
	10 g/l SDS	Carl Roth GmbH
Western blot buffer (10x)	12.1 g/l TRIS	Carl Roth GmbH
	30 g/l glycine	Carl Roth GmbH
	1 g/l EDTA	Carl Roth GmbH
	1 g/l NaN3	Carl Roth GmbH
Westernblot wash buffer (10x)	5 g/l Tween20	Carl Roth GmbH
	90 g/l NaCl	Carl Roth GmbH
	100 ml/l 1M TRIS pH7.4	Carl Roth GmbH
Collagen onplants for CAM (25 onplants)	75 µl 10 x MEM	Sigma Aldrich
	339.7 µl rat-tail collagen	Sigma Aldrich
	7.5 µl HEPES	PAN Biotechnology
	NaOH to neutralize pH	Carl Roth GmbH
	~250 µl conditioned medium	

3.2 Ethical approvals

All procedures involving human subjects were approved by the Institutional Review Board of the Medical University of Graz. Animal studies were carried out in line with the European Community's Council Directive.

3.3 Cell culture

3.3.1 Isolation of peripheral blood mononuclear cells (PBMC) and polymorphonuclear leukocytes (PMNL) from healthy donors

From healthy donors 70 ml of whole blood were collected in previously prepared tubes containing 3.8 % sodium citrate (1:10) to prevent coagulation and spun down at 400 x g for 20 min with low brake. Donors were selected independently of sex and age, however, it was noted whether a symptomatic allergy persisted. The platelet-rich plasma was aspirated and 6 ml of 6% dextran was added to remaining blood cells, filled up to 50 ml with 0.9 % saline solution and incubated at RT for 30 min to facilitate erythrocyte sedimentation. The upper phase after dextran sedimentation was transferred carefully onto 15 ml of histopaque and spun at 400 x g for 20 min with low brake. This density-gradient centrifugation step separates peripheral blood mononuclear cells (PBMCs) containing B- and T-lymphocytes as well as NK cells and monocytes from polymorphonuclear leukocytes (PMNL) containing granulocytes. PBMCs were collected from buffy coats found on top of Histopaque while PMNL are found in the cell pellet.

3.3.2 Generation of human monocyte-derived macrophages

PBMCs obtained from buffy coats were counted with a haemocytometer, resuspended in pre-warmed adhesion medium at a concentration 10 Mio cells/ml and seeded onto CellBind plates (6-well plate: 2 ml cell suspension/well, 12-well plate: 1 ml cell suspension/well) for 1.5 h at 37 °C in humidified atmosphere with 5 % CO_2. Subsequently, non-adherent cells were aspirated, the wells were washed three times with 1 ml wash buffer leaving ~1-2 Mio monocytes/well and differentiation medium containing 10 % FCS, 1 % P/S and 20 ng/ml rh-M-CSF (6-well plate: 2 ml/well, 12-well plate: 1 ml/well) was added. Differentiation medium

was changed every 2 – 3 days until macrophages were fully differentiated (day 6 – 8) which was determined by observing the cells' morphology.

3.3.3 Human monocyte-derived macrophage polarization to M1 and M2 phenotype

Following *in vitro* differentiation of monocytes, differentiation medium was replaced by activation medium without rh-M-CSF. To acquire classically activated macrophages with M1 phenotype, MDM were incubated for 48 h with activation medium supplemented with 20 ng/ml rh-INF-y and 100 ng/ml LPS. To obtain macrophages with M2 phenotype, the medium was supplemented with 20 ng/ml rh-IL-4 and MDM were incubated for 48 h. Additionally, MDM were incubated with activation medium without supplements to maintain the resting phenotype.

3.3.4 Stimulation of MDM with PGD_2 for CAM experiment

Monocytes were seeded in 6-well plates (20 Mio PBMC/well) and cultured with rh-M-CSF until fully differentiated to MDM. Differentiation medium was replaced with incomplete medium containing 2.5 % FCS and 1% P/S. Macrophages were stimulated with PGD_2 (1 µM, 300 nM, 100 nM, vehicle) twice a day (morning/evening) for 48 h. After 48 h stimulation the supernatant (SN) was collected and stored at -70 °C. One ml incomplete medium w/o supplements was added to each well and MDM were incubated for further 6 h. This SN was again collected and stored at -70 °C.

3.3.5 Collecting conditioned medium from activated and homeostatic monocytes for PGD_2-MOX ELISA

Monocytes were separated from PBMC using differential adhesion on CellBind 12-well plates. Cells were washed at least 4 – 5 times with washing buffer and cultured in monocyte activation medium (2.5 % FBS, 1 % P/S in RPMI with stable glutamine). Three conditions were tested; therefore, monocytes were incubated with medium only, 4 wells were classically activated with 20 ng/ml r-INF-y and 100 ng/ml LPS and 4 wells with rh-IL-4. Conditioned medium was collected 4, 8, 24 and 48 h post activation of cells and stored at -70 °C. Cells remaining were scraped off the bottom of the well by adding 100 µl protein

lysis buffer (10 mM Hepes, 1 mM EDTA, 1 % Triton-X, 1mM sodium-orthovanadate, 7.5µl/ml protease inhibitor) and stored at -70 °C.

3.3.6 Collecting MDM, M1 and M2-conditioned medium for PGD_2-MOX ELISA

Monocytes were differentiated into macrophages in 12-well plates (10 Mio PBMC/well) for 6 – 8 days. Subsequently, MDM in four wells were incubated in 1 ml activation medium w/o supplements to sustain a resting phenotype while four wells were classically activated with 20 ng/ml rh-INF-y and 100 ng/ml LPS and 4 wells with rh-IL-4. Conditioned medium from MDM, M1 and M2 macrophages was collected 4, 8, 24 and 48 h after activation start and stored at -70°C. Remaining cells were scraped off the bottom of the well by adding 100 µl protein lysis buffer (10mM Hepes, 1 mM EDTA, 1 % Triton-X, 1 mM sodium-orthovanadate, 7.5 µl/ml protease inhibitor) and stored at -70°C.

3.4 Flow Cytometry

HPGDS expression was investigated in macrophages and peripheral blood leukocyte subsets by indirect fluorescent staining of HPGDS and additional staining with fluorescently labelled antibodies against cell surface markers. Samples were analysed by flow cytometry using FACS Canto II from BD Bioscience. For samples stained with more than one fluorophore-conjugated Ab, a cell-based compensation was performed with FACS Diva Software. Raw data extracted from FACS Canto II were evaluated using FlowJo Diagnostic Software version 10.

3.4.1 Verification of successful macrophage activation with phenotype-specific markers CD80 and CD206

Fully differentiated and activated macrophages were washed twice with washing buffer and, subsequently, incubated for 15 min at 37°C with 1 ml accutase to facilitate cell detachment. MDM, M1 and M2 macrophages were collected in 15 ml falcon tubes by gently scraping off the cells from the bottom of the well and wells were washed once with 1 ml washing buffer. From one well of a 6-well plate approximately 1 - 2 million macrophages were collected and aliquots of 125 000 - 250 000 cells/ FACS tube were pre-fixed for 30 min in CellFix solution. All incubation steps were performed in the dark at RT followed by washing with 300µl PBS^-/tube and centrifugation for 7 min at 600 x g. Macrophages were

stained for alternatively activated macrophage cell surface markers CD80 and CD206 or with an isotype-matched control antibody. The PE-labelled monoclonal antibodies were used at a concentration of 20 µg/mL and incubated with cells for 30 min. Macrophages were fixed and permeabilized for 20 min followed by 10 min incubation in 1x permeabilization buffer and after a final washing step resuspended in 200 µl CellFix solution.

3.4.2 HPGDS staining in macrophages and immune cells in PBMC or PMNL fraction of peripheral blood

Peripheral blood monocytes, $CD4^+$ and $CD8^+$ T cells, Natural Killer (NK) cells, NK-T cells and B-cells were stained in the PBMC fraction obtained after density gradient centrifugation. Peripheral blood granulocytes, eosinophils and neutrophils, were stained in the PMNL fraction. Cells were washed once in 5 ml PBS without Ca^{2+} and Mg^{2+} (PBS^{--}), spun down for 7 min at 400 x g. The pellet was resuspended in PBS^-, divided up at 3 Mio cells in 100µl in one FACS tube and spun down again.

Table 1 Characterization of circulating immune cells by flow cytometry

	GATE	MARKER	BLOCKING	2^{ND} AB
MDM	-	-	UV-block/ 5 % FCS in PBS	1/2000
M1 MACROPHAGES	-	CD80	UV-block/ 5 % FCS in PBS	1/2000
M2 MACROPHAGES	-	CD206	UV-block/ 5 % FCS in PBS	1/2000
MONOCYTES	PBMC/ Monocytes	$CD14^+$	UV-block/ 5 % FCS in PBS	1/20 000
EOSINOPHILS	PMNL/ Granulocytes	$CD16^-$	FcX block	1/5000
NEUTROPHILS	PMNL/ Granulocytes	$CD16^+$	FcX block	1/5000
$CD4^+$ T CELLS	PBMC/ Lymphocytes	$CD3^+$ $CD4^+$	FcX block	1/5000
$CD8^+$ T CELLS	PBMC/ Lymphocytes	$CD3^+$ $CD8^+$	FcX block	1/5000
NK/T CELLS	PBMC/ Lymphocytes	$CD3^-$ $CD56^+$	FcX block	1/5000
NK CELLS	PBMC/ Lymphocytes	$CD3^+$ $CD56^+$	FcX block	1/5000
B CELLS	PBMC/ Lymphocytes	$CD19^+$ $CD20^+$	FcX block	1/5000
PLASMA CELLS	PBMC/ Lymphocytes	$CD138^+$	FcX block	1/5000

All incubation steps were performed in the dark at RT followed by washing with 300µl PBS^{--} /tube and centrifugation for 7 min at 400 x g. To differentiate between immune cells PBMCs were stained for 15 min at RT with cell-specific surface markers coupled to fluorescent dyes listed in Table 1. Macrophages were collected as described for activation control and successfully activated macrophages were used for HPGDS staining. 125 000 - 250 000 macrophages/ FACS tube were pre-fixed for 30 min in fixation buffer followed by further staining steps as described for immune cells.

Following centrifugation cells were incubated for 30 min with a blocking reagent - monocytes with a 1:1 mixture of UV-block (BD Bioscience) and 5% FCS in PBS^{-} - and other cells with FcX-receptor block (BioLegend), to prevent non-specific binding. Cells were incubated for 30 min in 100µl 1:100 dilution (5 µg/ml) of primary monoclonal mouse anti-human HPGDS antibody (Novus Bioscience) or the corresponding isotype control (mouse IgG) in permeabilization buffer as recommended, followed by incubation for 30 min with secondary antibody AF488-coupled rabbit anti-mouse IgG. After two washing steps cells were resuspended in 250 µl fixation buffer. Controls performed for each experiment include untreated cells (no fixation, permeabilization or staining), an unstained control and cells stained for surface markers only (AF488 unstained) and secondary antibody only to evaluate reliability of staining.

3.5 $CD14^{+}$ monocyte isolation from PBMC fraction of peripheral blood

Classical $CD14^{+}$ monocytes were isolated from peripheral blood by negative selection with help of the magnetic-activated cell sorting (MACS)-based monocyte isolation kit II from Miltenyi. 100 million PBMCs were used as starting point of the isolation and steps were performed according to the protocol. Between 5 to 10 million monocytes could be isolated from 100 million PBMCs with a purity from 85 % to 95 %. Cells were divided into two fractions, while one was resuspended in 600 µl TriReagent for RNA extraction and RT-qPCR and the other part was resuspended in 250 µl protein lysis buffer and aliquoted for Western blot analysis.

3.6 Detecting HPGDS in monocytes and macrophages on protein level by western blotting

Cell lysates of MDM, M1 and M2 macrophages from healthy donors were collected from one well of a 6-well plate (~ 1 – 2 x 10^6 cells), respectively, by addition of 120 µl protein lysis buffer and scraping off cells. Lysates were vortexed for 10 min at 4 °C, spun down at 12 000 rpm for 10 min at 4°C and the supernatant was aliquoted and transferred to new Eppendorf tubes and stored at -70 °C until further use. Additionally, protein lysates from monocytes isolated with help of the Miltenyi monocyte isolation kit II were used for Western blot analysis of HPGDS expression.

For Western blotting, protein lysates (20 µl) were defrosted on ice and a SDS PAGE performed. 6x sample buffer was added and samples were boiled (95 °C) in a heating block for 5 min. Twenty µl of boiled samples were loaded onto a precast gel (4-20 %) and in the first and last lane 5 µl of a pre-stained protein ladder were added. The gel was run at 125 V for 1.5 h, then washed for 15 min in blotting buffer and transferred to the pre-assembled tray. A PVDF membrane (0.2 µm) was activated for 5 min in MeOH, washed for 15 min in blotting buffer and put on top of the SDS PAGE gel. Proteins were transferred onto the PVDF membrane by wet blotting (on ice) at 100 V for 1 h. To check whether proteins were transferred successfully the membrane was shortly stained with Ponceau red. Subsequently, the membrane was incubated with 5 % - milk in washing buffer on a shaker at RT for 1 h to block non-specific binding followed by incubation with primary mouse anti-human HPGDS Ab (0.25 µg/ml) in 1 % milk in washing buffer at 4 °C o/n. Next day, the membrane was washed four times for 15 min in washing buffer and incubated with horseradish peroxidase-conjugated secondary goat anti-mouse Ab (1/5000 in 1% milk) for 1.5 h. The membrane was washed four times for 15 min with washing buffer on the shaker and bands were visualized by incubation for 5 min with Clarity™ Western ECL Blotting Substrate (BioRad) and subsequently evaluated with a BioRad chemiluminescence detector. After detection, the membrane was washed for 15 min at RT with stripping buffer (Restore PLUS Western blot stripping buffer, ThermoScientific), blocked for 30 min at RT with 5 % milk and subsequently incubated with primary GAPDH and corresponding secondary Ab. HPGDS expression was determined from 6 healthy donors and normalized to GAPDH (Primary Ab rabbit anti-human GAPDH, 1/3000; Secondary Ab goat anti-rabbit 1/5000).

3.7 Detecting HPGDS in monocytes and macrophages on mRNA level by RT-qPCR

Homeostatic MDM, M1 and M2 macrophages (1-2 Mio per well) were collected in 200 µl TriReagent reagent and stored at -70°C until further use. Additionally, monocytes isolated with Miltenyi kit were used for RNA extraction and RT-qPCR.

For RNA isolation samples were thawed on ice and additional 400 µl TriReagent were added. Phases were separated with 120 µl chloroform for 3 min at RT and centrifugation at 12 000 rpm for 15 min at 4°C. Upper aqueous phase containing RNA was transferred to a new tube and precipitation was induced by adding 99.9% EtOH. Samples were further purified with a RNeasy Mini Kit (Quiagen) according to the protocol and RNA was eluted in 30 µl RNAse-free water with 2 µl Protector RNase Inhibitor (Roche). RNA concentration was determined with a nanodrop and 1 µg RNA was reverse transcribed using the iScript cDNA Synthesis Kit (BioRad) with a thermal cycler using the suggested protocol (5 min at 25°C, 20 min at 46°C, 1 min at 95°C). A reverse transcription control was performed by mixing 1 µl RNA from 4 randomly chosen samples, adding the reaction mix but no reverse transcriptase. The 20 µl reaction mix from cDNA synthesis was diluted with 100 µl RNAse free water and for subsequent qPCR a 1:10 dilution of these samples was used in the reaction. HPGDS and GAPDH as housekeeping gene were detected using validated BioRad primers and a SYBR green reaction mix by evaluating the number of cycles needed to reach the threshold line (Ct). DeltaCt values for the HPGDS gene were calculated by subtracting corresponding HPGDS Ct by GAPDH Ct values. Additionally, a negative control (ddH_2O) and reverse transcription control were performed and confirmed by qPCR. Results are shown from 6 biological and 2 technical replicates.

3.8 PGD_2 production by murine alveolar macrophages

We wanted to assess whether alveolar macrophages in naïve mice, an allergic ovalbumin (OVA)-induced mouse model and an LPS-induced mouse model of acute lung injury produce PGD_2. To elucidate PGD_2-production potential under these conditions alveolar macrophages were collected by broncho-alveolar lavage, which was performed by Katharina Jandl, and subsequent culture for 4 and 18 hours to allow collection of conditioned medium.

3.8.1 Ovalbumin (OVA)-induced allergic airway inflammation

Allergic lung inflammation was induced in 3-month old BALB/c mice (n = 5) by immunization with ovalbumin (OVA). 10 µg of OVA adsorbed to $Al(OH)_3$ was injected i.p. on days 0 and 7. Mice were challenged by an OVA-aerosol in saline on days 14 and 16. Alveolar macrophages were collected by broncho-alveolar lavage fluid on day 17.

3.8.2 LPS-induced acute lung injury (ALI)

Acute pulmonary inflammation was induced in 3-month-old BALB/c mice (n = 5) by intranasal application of 1 mg LPS/kg body weight. Before LPS application mice were lightly anesthetized by intra peritoneal injection of 120 µl Ketamine/Xylazine (10 mg/ml Ketasol, 1 mg/ml Rompun in saline) solution. LPS solution was added dropwise to nostrils of mice to be inhaled. Broncho-alveolar fluid was collected 4 hours after LPS application.

3.8.3 Broncho-alveolar lavage (BAL) fluid collection and culturing of AM

OVA mice (n = 5), ALI mice (n = 5) and naïve mice (3-month-old BALB/c mice, n = 5) were anesthetized with an overdose (600 - 700 µl) of Ketamine/Xylazine solution. Thorax was opened, trachea exposed and a tracheal cannula (1.20x40mm needle) inserted and fixed with a thread. The lung was lavaged 8-times with 1 ml ice cold BAL buffer (PBS^- + 0.6 mM EDTA) and collected in a Falcon tube on ice. BAL fluid was spun down at 400 x g for 5 min at RT and resuspended in 1 ml BAL buffer. Erythrocytes were lysed by adding 5 ml of NH_4Cl_2 on ice (15 min). Then cells were washed with 5 ml BAL buffer followed by centrifugation at 400 x g for 5 min and cells were resuspended in 1 ml BAL buffer. The number of viable cells was evaluated by counting isolated cells with Trypan blue. Additionally, alveolar macrophages were morphologically identified and the ratio of alveolar macrophages to total cells was determined. Cells were resuspended in macrophage adherence medium to get a final concentration of 0.3 Mio alveolar macrophages/ml. Subsequently, 150 000 alveolar macrophages from ALI and OVA or 75 000 alveolar macrophages from naïve mice per well were seeded in a 48-well plate (Costar CellBind). After 1.5 h incubation at 37°C non-adherent cells were washed off (3 x 500 µl wash buffer) and medium was replaced by activation medium (RPMI, 10 % FBS, 1 % P/S). Cells were cultured at 0.15 Mio macrophages/ml medium. Conditioned medium was collected after 4 and 18 hours and amount of PGD_2 released by macrophages was evaluated with a MOX-PGD_2 ELISA kit (Caymen).

3.9 PGD_2-Methoxime (MOX) ELISA

The PGD_2-MOX ELISA kit uses a methyloximating reagent (methoxylamine-HCl) to generate a stable PGD_2-methoxime derivative, which enables reliable detection. Samples collected for PGD_2 measurement were defrosted quickly and mixed at a 1:1 ratio with the freshly prepared methyl oximating reagent (0.1 g methoxylamine HCl, 0.82 g sodium acetate in 10 ml 1:9 solution of EtOH:water). After vortexing, samples were heated at 60°C for 30 min and stored at -20°C until assaying. PGD_2-MOX ELISA was performed as stated in corresponding booklet including 2 non-specific binding wells (50 µl ELISA buffer + 50 µl MOX-medium), 2 maximum binding wells (B_0) and a PGD_2-MOX standard dilution assayed in duplicates ranging from 2.0 pg/ml to 250 pg/ml. The standard as well as samples were diluted in MOX-medium (1:1 mixture of RPMI with 10 % FBS, 1 % P/S and methyl oximating reagent) and assayed in duplicates at adequate dilution. Additionally, methoximated PGE_2, TBX_2 and medium containing supplements was tested to exclude non-specific binding. ELISA plates were incubated with samples, tracer and anti-serum at 4°C over night. Next day wells were washed 5 times with wash buffer using a microplate washer and subsequently incubated with 200 µl Ellman's reagent for 90 min at RT on a shaker in the dark and evaluated with a plate reader (BioRad) by measuring the absorbance at 410 nm.

3.10 Bicinchoninic acid (BCA) assay for protein concentration determination

Cell lysates from all wells with monocytes and macrophages for PGD_2 production were collected in 100 µl protein lysis buffer, in parallel with conditioned medium collection and stored at 70°C. Lysates were thawed by vortexing at 4°C for 30 min, spun down at 14 000xrpm for 10 min and supernatant was transferred into a new tube. Protein content in these samples was determined by means of a BCA assay. A bovine serum albumin (BSA) standard curve (0 - 1500 µg protein/ml) was prepared and assayed in duplicates. A 1:2 dilution of all samples was assayed in duplicates (10 µl), while the ratio between working reagent and samples/standard was 1:20. The plate was incubated at 37°C for 30 min and, subsequently, the absorbance at 562 nm was measured to determine protein concentration. Obtained mean values of protein content per well were used for normalization of PGD_2 values from the MOX-PGD_2 ELISA.

3.11 Chicken chorioallantoic membrane (CAM) angiogenesis assay

The chicken CAM angiogenesis assay uses the chorioallantoic membrane, which is the respiratory organ during development in the egg, of 10-day-old chicken embryos. Deryugina et.al. described in great detail how to perform the assay using CAM collagen onplants [82]. Fertilized chicken eggs were obtained (Schropper GmbH, A-2640 Gloggnitz – Aue) and at day 3 the egg shell was carefully cut using a portable drill. The content of the egg was transferred to a sterile plastic weigh box and incubated for additional 7 days at 37°C and 75 % relative humidity. The embryos were incubated *ex ovo* to avoid pro-inflammatory effects of shell dust. On day 10 the CAM is developed enough to carry collagen onplants and sustain angiogenesis. Double-gridded sandwiches were prepared using 3x3 mm nylon grids with 2x2 mm nylon grids on top, sterilized by UV-radiation prior to collagen mix addition. A mastermix for collagen onplants was prepared on ice containing 2 mg/ml collagen, which was divided up depending on groups tested and mixed with conditioned medium pooled from 4 donors to reach the final volume. Subsequently, 30 µl of prepared collagen mixtures were added to nylon sandwiches and these were incubated for 1 h at 37°C to facilitate collagen polymerization. For each experiment, 6 eggs with 6 onplants placed onto the CAM were used for different conditions. The chicken embryos were incubated for further 3 days and angiogenic properties of samples were evaluated on day 13 by counting positive panels showing small vessels that have grown into the nylon grid sandwich. Positive panels were counted by a blinded operator not familiar with tested substances.

3.12 Statistical Analysis

All data are shown as mean ± standard error of the mean (SEM) for n observations as indicated unless stated otherwise. Statistical analyses were performed with GraphPad Prism5 software using a suitable test (Student's t-test for 1 variable and 2 groups, one-way ANOVA for 1 variable and more than 2 groups or two-way ANOVA for ≥ 2 variables and groups). Additionally, for ANOVA analyses a Bonferroni post-test was conducted (*$p<0.05$, **$p<0.01$, ***$p<0.001$).

4 Results

First, we were interested in finding potential PGD_2 sources in acute lung injury, whereby there was already a strong link to macrophages. The hematopoietic PGD_2 synthase (HPGDS) is the rate-limiting enzyme of PGD_2 production in peripheral tissues and constitutive expression of this enzyme comprises a first clue on potential PGD_2 sources amongst leukocytes in the lung. Therefore, we characterized HPGDS expression in human monocytes and monocyte-derived macrophages (MDM) on protein and mRNA level as well as PGD_2 secretion under homeostatic and activated conditions. Additionally, peripheral blood leukocyte subsets were screened for HPGDS expression with a flow cytometric approach to investigate possible other PGD_2 sources. Besides PGD_2 secretion by immune cells in inflammation, it is crucial to investigate how this potent mediator influences lung pathology including angiogenesis. To this end, preliminary experiments were conducted on whether activated DP1 and DP2 receptors on MDM influence secretion of pro- or anti-angiogenic factors by macrophages.

4.1 PART I – HPGDS is selectively upregulated during human macrophage differentiation *in vitro*

4.1.1 Human peripheral blood monocytes differentiate into macrophages *in vitro* and can be further activated to M1 and M2 phenotype

Separation of peripheral blood monocytes from healthy donors was achieved by exploiting the differential adhesion characteristics between PBMCs, whereby, monocytes adhere more readily to cell culture plates. This allows washing off lymphocytes only and leaves an enriched cell layer of adherent monocytes. A schematic representation of MDM generation and activation is shown in Figure 5a. Monocytes were then incubated with differentiation medium containing 20 ng/ml M-CSF, which was changed every 2-3 days.

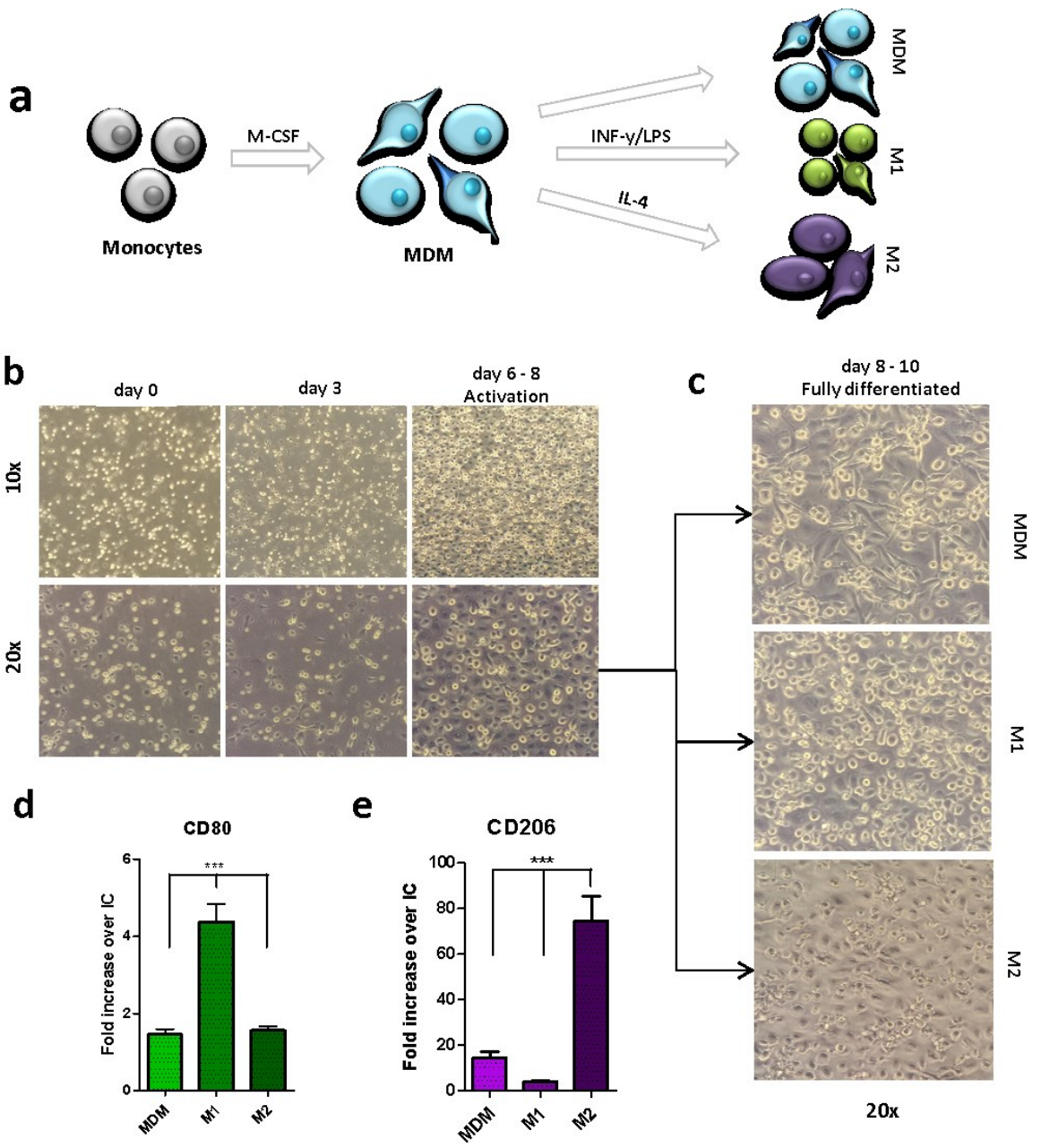

Figure 5. Generation and characterization of human monocyte-derived macrophages (MDM). (a) Schematic representation of generation and activation of human MDM. (b) Representative images at 10x and 20x magnification of macrophage differentiation *in vitro* starting at day 0 with seeded monocytes, first morphological changes on day 3 in culture and fully differentiated MDM at day 6-8. There is an approximate balance between spindle- and oval-shaped cells. (c) Representative images of homeostatic MDM, M1 and M2 macrophages after 48 h activation. MDM keep the morphological balance between spindle- and oval-shaped cells, M1 macrophages are smaller and more compact while M2 macrophages have a slightly enlarged and flattened appearance. (d) CD80 is upregulated in INF-γ/LPS-stimulated MDM (M1). (e) CD206 is highly expressed in IL4-stimulated MDM (M2). (d and e n = 10; One-way ANOVA with Bonferroni post-test, *p<0.05, **p<0.01, ***p<0.001)

Fully differentiated human monocyte-derived macrophages (MDM) were identified morphologically by a balance between oval- and spindle-shaped cells (Figure 5b and c), which happened mostly after 6-8 days, but was donor-dependent. Subsequently, MDM were either cultured for 48 h in homeostatic state or activated to M1 or M2 macrophages by incubation with 100 ng/ml LPS and 20 ng/ml INF-γ or 20 ng/ml IL-4, respectively. Homeostatic MDM kept the balance of spindle and oval shaped morphology, while M1 macrophages typically were smaller and rounder and M2 macrophages showed enlarged, flattened morphology (Figure 5c). On day 8 – 10 macrophages were collected for flow cytometry, protein lysates or for RNA extraction. The activation status was confirmed by cell surface marker expression, whereby INF-γ/LPS-stimulated macrophages showed an average 4.4-fold increase normalized to the isotype control (IC) of CD80 fluorescence signal, a commonly used M1 macrophage marker, while the mannose receptor (CD206) signal was on average 74-fold increased by IL-4 stimulation to acquire M2 macrophages (Figure 5, d and e).

4.1.2 Peripheral blood monocytes do not express HPGDS

To start with, we wanted to assess whether HPGDS, the major PGD_2-producing enzyme in peripheral tissues and cells of the hematopoietic lineage, is expressed in monocytes as they may also contribute to elevated PGD_2 levels. A flow cytometric approach was chosen and, thus, monocytes were stained with anti-human HPGDS or an isotype control (IC) and an AF488-conjugated secondary Ab in the peripheral blood mononuclear cell (PBMC) fraction from symptomatic allergic or healthy donors. CD14 positive monocytes were selected from the monocyte gate of PBMCs (Figure 6a) and the geo-mean fluorescence intensity was evaluated. The secondary Ab concentration was titrated and for all following experiments with monocytes a dilution of 1/20 000 was chosen (Figure 6b). To assess HPGDS expression in cells, fold increase of HPGDS Ab stained cells over isotype control was calculated. Only a slight increase in geo-mean signal in HPGDS stained samples could be detected, indicating negligible HPGDS expression in circulating monocytes, which was also confirmed by evaluation of the percentage of positive cells (Figure 6b,c).

Results obtained for monocytes are displayed as reference for HPGDS expression in macrophages (Figure 7 and 8).

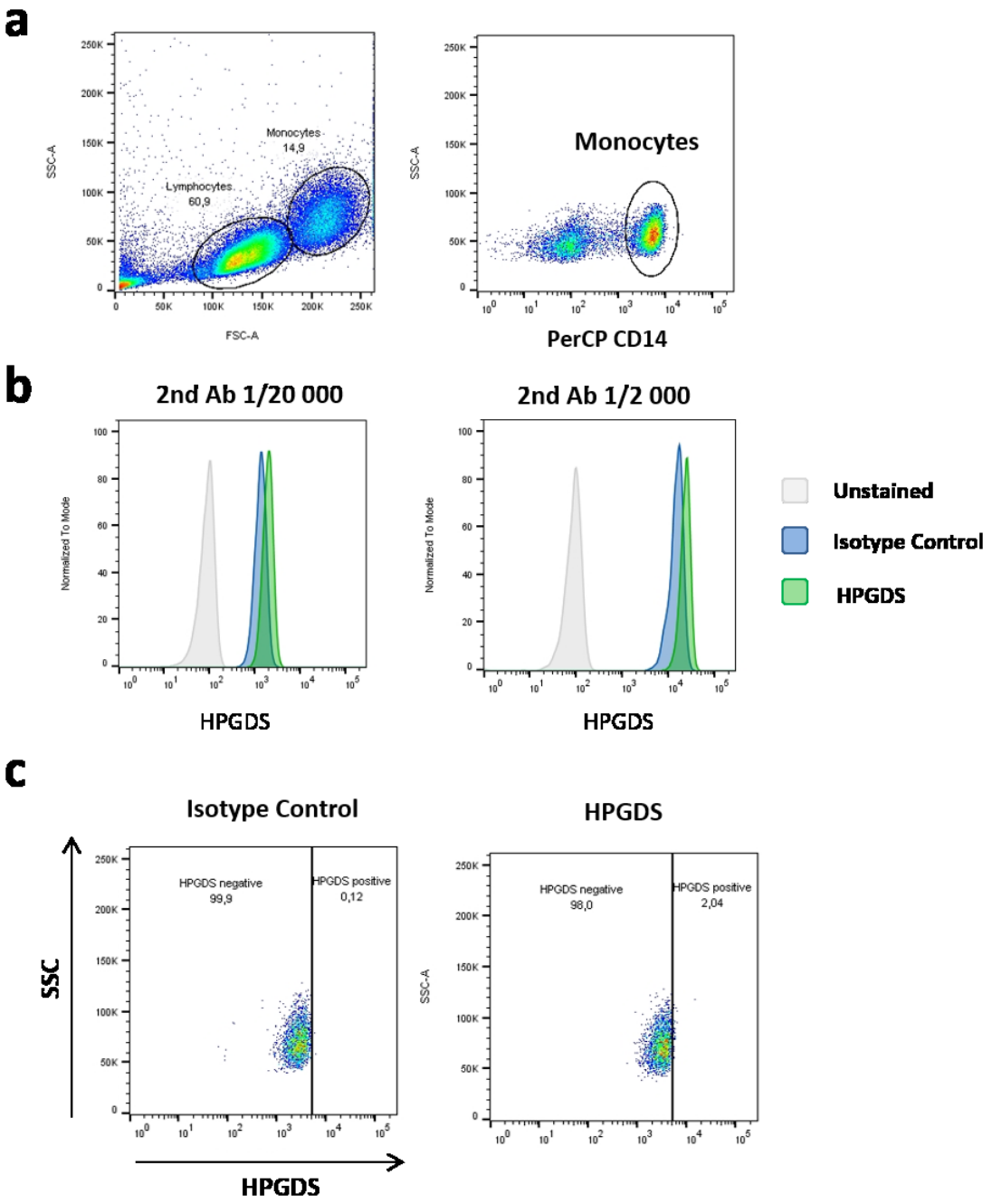

Figure 6. Peripheral blood monocytes do not express HPGDS. (a) Gating strategy to identify monocytes in PBMC. $CD14^+$ monocytes were selected from the monocyte region of PBMCs. (b) Hardly any signal increase could be observed in HPGDS-Ab stained population. After 2° Ab titration all experiments with monocytes were performed with a 2° Ab dilution of 1/20 000 as no difference could be seen as compared to 1/2 000. (c) Between 1-2 % of monocytes were positive for HPGDS.

4.1.3 HPGDS is selectively upregulated during macrophage differentiation *in vitro*

As HPGDS-positive cells, which have morphologically been identified as macrophages, have been shown to be increased in ARDS patients, the next step was to confirm that human monocyte-derived macrophages (MDM) express HPGDS as well as to investigate potential differences between M1 and M2 phenotypes.

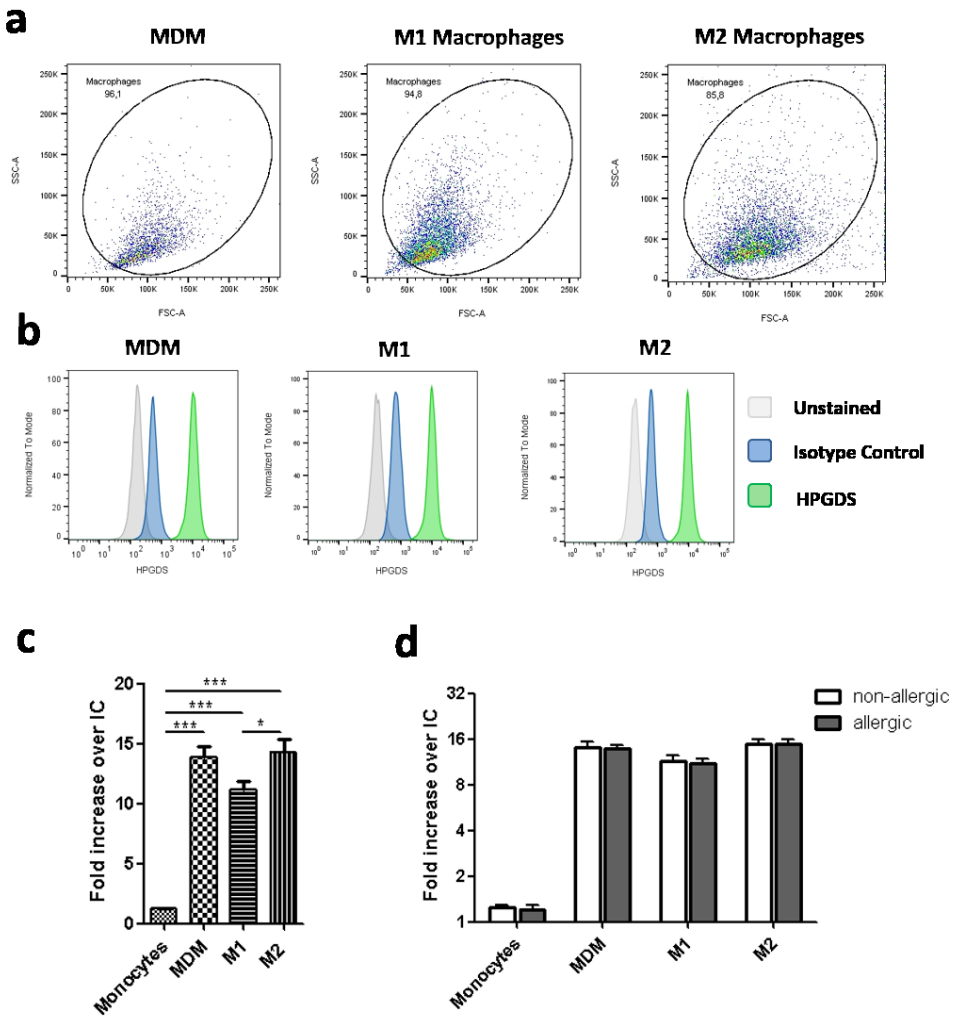

Figure 7. HPGDS is upregulated during macrophage differentiation in vitro. HPGDS expression was determined 48 h after activation by flow cytometry and immunological staining. (a) Characteristic FSC/SSC dot plots of MDM, M1 and M2 macrophages. M1 macrophages were more compact and have a lower FSC, while M2 macrophages have and increased FSC. (b) MDM, M1 and M2 macrophages show a distinct increase in fluorescence intensity in comparison to isotype control. Graphs are representative for 10 independent experiments. (c) In comparison to monocytes, there is a significant increase of HPGDS in all three macrophage phenotypes. M1 macrophages showed a smaller fold increase. (n = 10, mean ± SEM, One-way ANOVA with Bonferroni post-test, (*p<0.05, **p<0.01, ***p<0.001) (d) HPGDS expression in monocytes and macrophages does not differ in symptomatic allergic and healthy donors. (n = 5, mean ± SEM, Two-way ANOVA with Bonferroni post-test, *p<0.05, **p<0.01, ***p<0.001)

Human MDM were differentiated from peripheral blood monocytes as described earlier and cells were collected 48 hours after activation.

Subsequently, macrophages were divided up so that an activation control staining with CD80 as M1 and CD206 as M2 marker could be performed in parallel to HPGDS staining (see also Figure 5 d and e). MDM, M1 and M2 macrophages were stained with anti-HPGDS Ab or IC and as control left unstained or with 2° Ab only. HPGDS expression was evaluated by flow cytometry, whereby macrophage populations were selected upon their characteristic forward scatter (FSC) and side scatter (SSC).

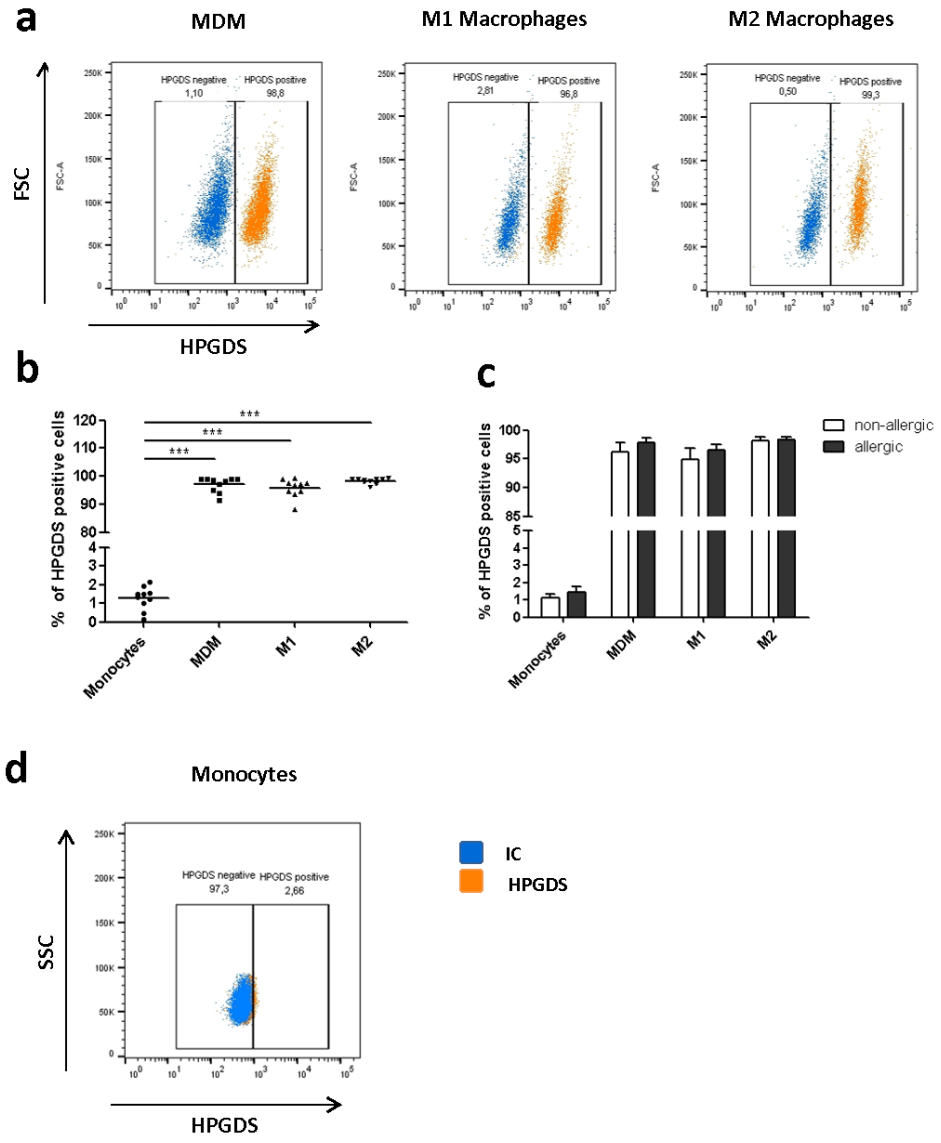

Figure 8. Human MDM express HPGDS under homeostatic and activated conditions. HPGDS expression was evaluated by flow cytometry and in comparison to a mouse IgG1 isotype control. (a and d) Evaluation of HPGDS positive cells with help of isotype control. (b) Resting and activated human MDM are expressing HPGDS, while only a small percentage of monocytes express HPGDS. (n = 10, mean ± SEM, One-way ANOVA with Bonferroni post-test, (*p<0.05, **p<0.01, ***p<0.001) (c) There is only a small tendency of increased HPGDS expression in allergic subjects, (n = 5, mean ± SEM, One-way ANOVA with Bonferroni post-test, (*p<0.05, **p<0.01, ***p<0.001)

M1 macrophages showed a smaller, more compact shape which resulted in lower FSC whereby M2 macrophages scattered wider and had a higher FSC than MDM and M1 (Figure 7a). Concerning the HPGDS staining, M2 macrophages had the highest fold increase (14.3) over IC, followed by 13.9-fold increase in MDM, 11.2-fold increase in M1 macrophages and 1.2-fold increase in peripheral blood monocytes.

A significant increase in HPGDS signal could be observed in all three macrophage phenotypes in comparison to monocytes, although to a lesser extent in M1 macrophages (Figure 7c). These results confirmed that HPGDS is upregulated during monocyte differentiation into macrophages *in vitro*. Additionally, donors were stratified into symptomatic allergic or non-allergic (n = 5) but no difference in HPGDS expression could be determined in monocytes, MDM, M1 and M2 macrophages (Figure 7d). Furthermore, determination of the percentage of HPGDS-positive cells allows identification of positive subsets within cell populations. Therefore, a gate was set with help of the isotype-stained sample to establish a cut-off to identify HPGDS positive cells. Representative images for macrophage populations are shown in Figure 8a and Figure 8d for monocytes. MDM, M1 as well as M2 macrophages were distinctly positive (95 – 95 %), whereby only a small percentage of monocytes (1 – 2 %) stained positive for HPGDS (Figure 8b). A closer examination of monocytes and MDM from symptomatic allergic and healthy donors showed no significant difference in the number of HPGDS positive cells, however, a small tendency for more HPGDS positive cells in allergic subsets (Figure 8c).

4.1.4 Relative HPGDS expression in MDM, M1 and M2 macrophages on protein and mRNA level

To further confirm that HPGDS is expressed in human macrophages and to validate flow cytometry outcomes, protein lysates from MDM, M1 and M2 macrophages after 48 h activation were collected and RNA was extracted.

In Figure 9a a representative Western blot from 2 donors is displayed, showing, a positive signal at 23 kDa for HPGDS in accordance with literature [1], in all three macrophage phenotypes. Normalization of HPGDS band peak volumes to GAPDH revealed that MDM showed the strongest signal which correlated to about 60 % of GAPDH expression, shortly followed by M2 macrophages with about 45 % of GAPDH (Figure 9b). The least amount of HPGDS could be detected in M1 macrophages after 48 h activation (~40 % of GAPDH), which is in agreement with flow cytometry results. In monocytes, no HPGDS could be detected, which further confirmed the results obtained with flow cytometry.

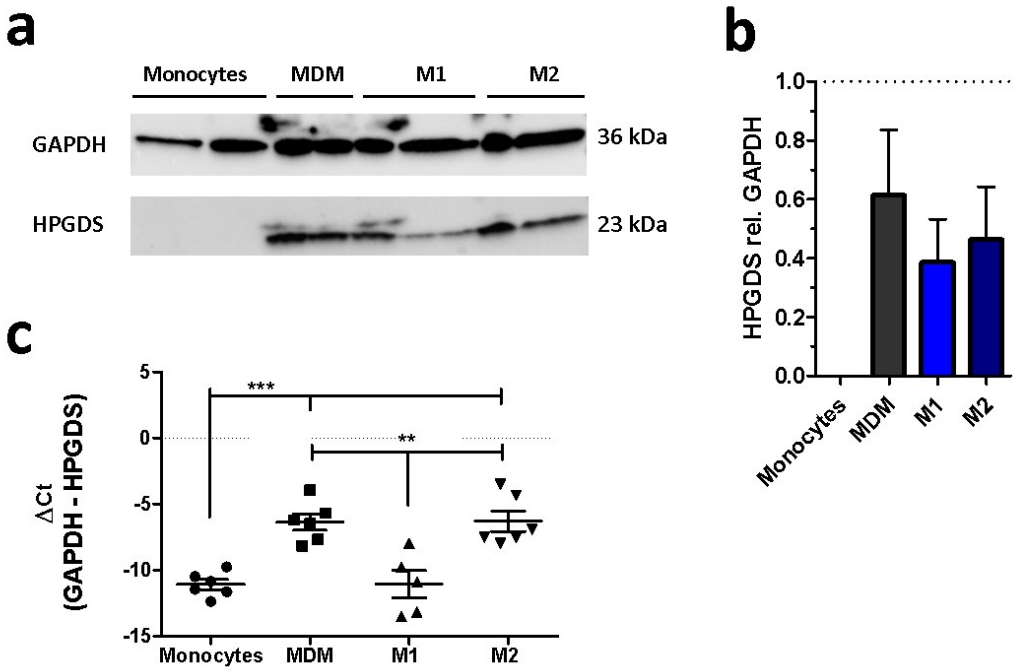

Figure 9. Relative HPGDS expression in monocytes and macrophages on protein and RNA level. (a) Immunoblot of anti-GAPDH and anti-HPGDS from 2 donors, representative for 6 donors. Membrane was stained for HPGDS, then stripped and subsequently stained for GAPDH. (b) Normalization of HPGDS signal to GAPDH signal. MDM show the highest HPGDS expression (~60 % of GAPDH expression), while in monocytes no HPGDS signal could be detected (n = 6, mean ± SEM) (c) RT-qPCR results for HPGDS cDNA normalized to GAPDH cDNA. HPGDS cDNA was present in all three macrophage phenotypes, however, at a very low level. Significantly more HPGDS mRNA was present in MDM and M2 macrophages in comparison to monocytes, however, no difference could be seen in M1 macrophages. (n = 5-6, mean ± SEM)

A RT-qPCR was performed to evaluate HPGDS mRNA levels in monocytes and macrophages whereby a semi-quantitative method was used. Ct values for HPGDS were extracted and normalized to corresponding Ct for the housekeeping gene GAPDH to yield ΔCt values. ΔCt values obtained for monocytes, MDM, M1 and M2 macrophages are displayed in Figure 9c. In all macrophage phenotypes, there was less HPGDS mRNA than GAPDH mRNA present, whereby M1 macrophages contained the least amount – on average about 32-times (2^5) less than MDM and M2 macrophages. In monocytes, the detectable mRNA level was comparable to the level in M1 macrophages.

4.2 PART II – Flow cytometric screening for HPGDS-expressing peripheral blood leukocyte subsets

We next set out to elucidate HPGDS expression in other circulating leukocytes, which may participate in inflammatory reactions.

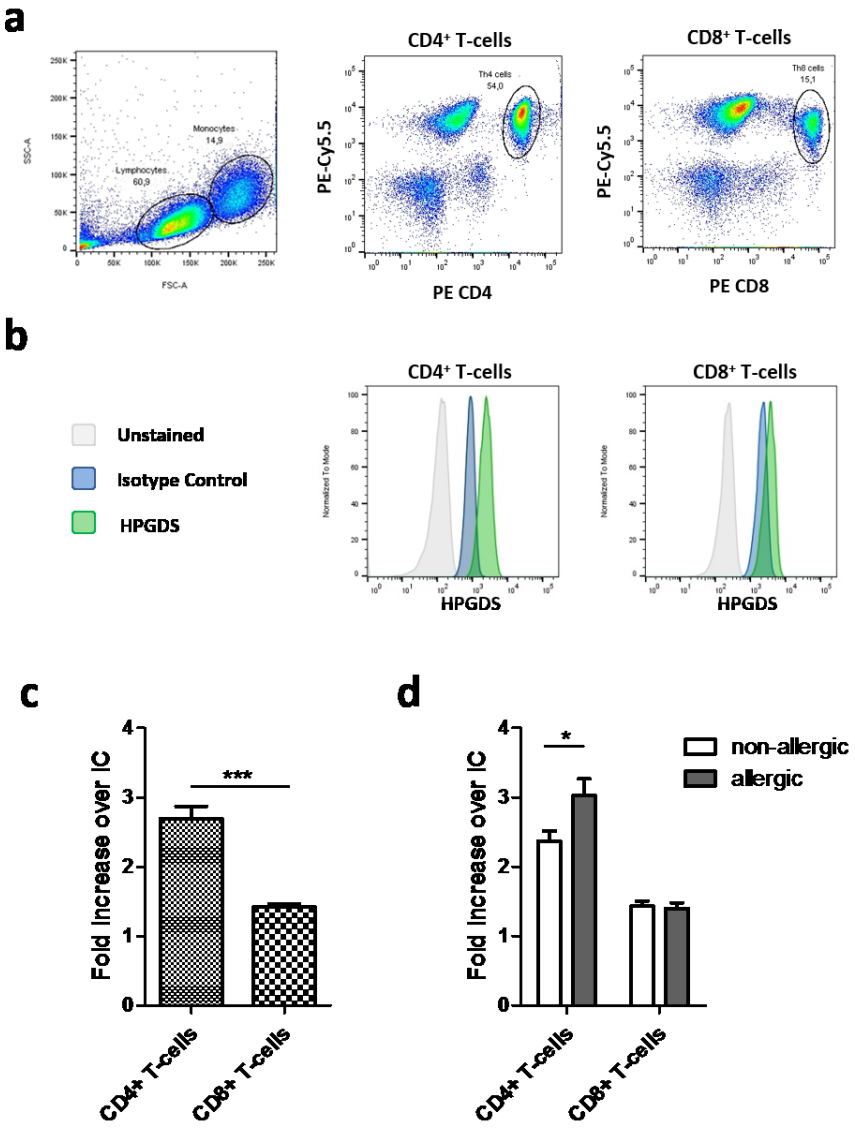

Figure 10. CD4⁺ T-cells express HPGDS more strongly than CD8⁺ T-cells. PBMCs from healthy donors were stained immunologically for HPGDS and analysed by flow cytometry. (a) Gating strategy for CD4 and CD8 positive T-cells. The lymphocyte gate of PBMCs was selected and CD3/CD4 or CD3/CD8 double positive cells were selected, respectively. (b) CD4⁺ T-cells have a higher HPGDS signal than CD8⁺ T-cells. (c) CD4⁺ T-cells have a significantly higher HPGDS signal fold increase over IC. (n = 10, mean ± SEM, Student's t-test, ***p<0.001). (d) In symptomatic allergic donors there is an increase in HPGDS-expression in CD4⁺ T-cells. However, no difference in CD8⁺ T-cells. (n = 5, mean ± SEM, Two-way ANOVA with Bonferroni post-test, (*p<0.05, **p<0.01, ***p<0.001)

4.2.1 CD4⁺ T-cells express HPGDS more readily than CD8⁺ T-cells.

Further, we wanted to assess whether peripheral blood CD4 and CD8 positive T-cells express HPGDS to gauge their potential for PGD_2 production. T-cells were stained in PBMC fraction of peripheral blood from healthy and symptomatically allergic donors, whereby CD3/CD4 or CD3/CD8 double-positive populations were selected (Figure 10a).

HPGDS expression was evaluated as described for monocytes by means of fold increase over isotype control and the percentage of positive cells. $CD4^+$ T-cells showed a significantly higher HPGDS fold increase over isotype control (2.7-fold increase) than $CD8^+$ T-cells with 1.4-fold increase. Interestingly, $CD4^+$ T-cells from allergic donors had a 3-fold increase over IC while non-allergic donors only a 2.4-fold increase over IC (Figure 10 c and d). No difference was seen between the two groups for $CD8^+$ T-cells (1.4-fold increase).

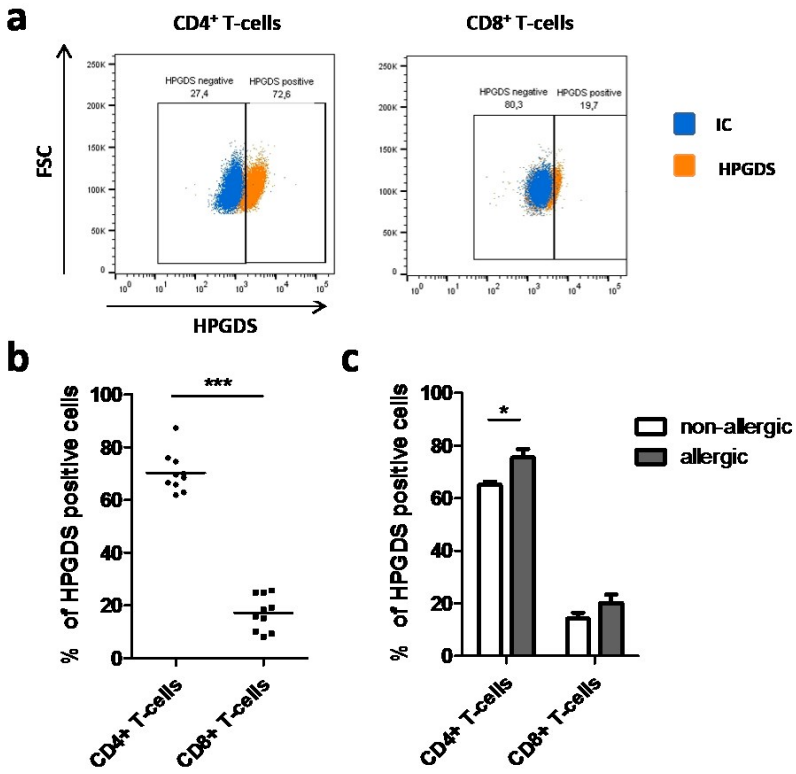

Figure 11. The majority of circulating $CD4^+$ T-cells is HPGDS positive. Flow cytometric analysis of HPGDS expression by immunostaining in PBMC fraction of peripheral blood. (a) Representative image of evaluation of HPGDS positive cells. $CD8^+$ T-cells show a small shift while two different population signals are visible for $CD4^+$ T-cells. (b) The majority (~70%) of $CD4^+$ T-cells is HPGDS positive, significantly more than $CD8^+$ T-cells. (n = 10, mean ± SEM, Student's t-test, ***p<0.001). (c) A higher percentage of $CD4^+$ T-cells was found in symptomatic allergics. Also a slight increase of HPGDS positive cells can be seen in $CD8^+$ cells. (n = 5, mean ± SEM, Two-way ANOVA with Bonferroni post-test, (*p<0.05, **p<0.01, ***p<0.001)

For further characterization, the percentage of HPGDS positive cells was determined by setting the cut-off geo-mean value with the help of the IC signal. Representative scatter dot plots of the percentage of HPGDS positive cells are displayed in Figure 11a and show that the majority of $CD4^+$ T-cells (70.3 %) but only 17.2 % of $CD8^+$ T-cells were HPGDS-positive (Figure 11b). Additionally, in non allergic donors 65.1 % of $CD4^+$ T-cells were HPGDS positive while in allergic donors even 75.5 % (Figure 11c). This indicates a potential role of PGD_2 production by $CD4^+$ T-cells in allergic conditions. Also in $CD8^+$ T-cells there is a tendency of increased HPGDS expression in allergic subjects visible (14.2 % vs. 20.2 % in allergic donors).

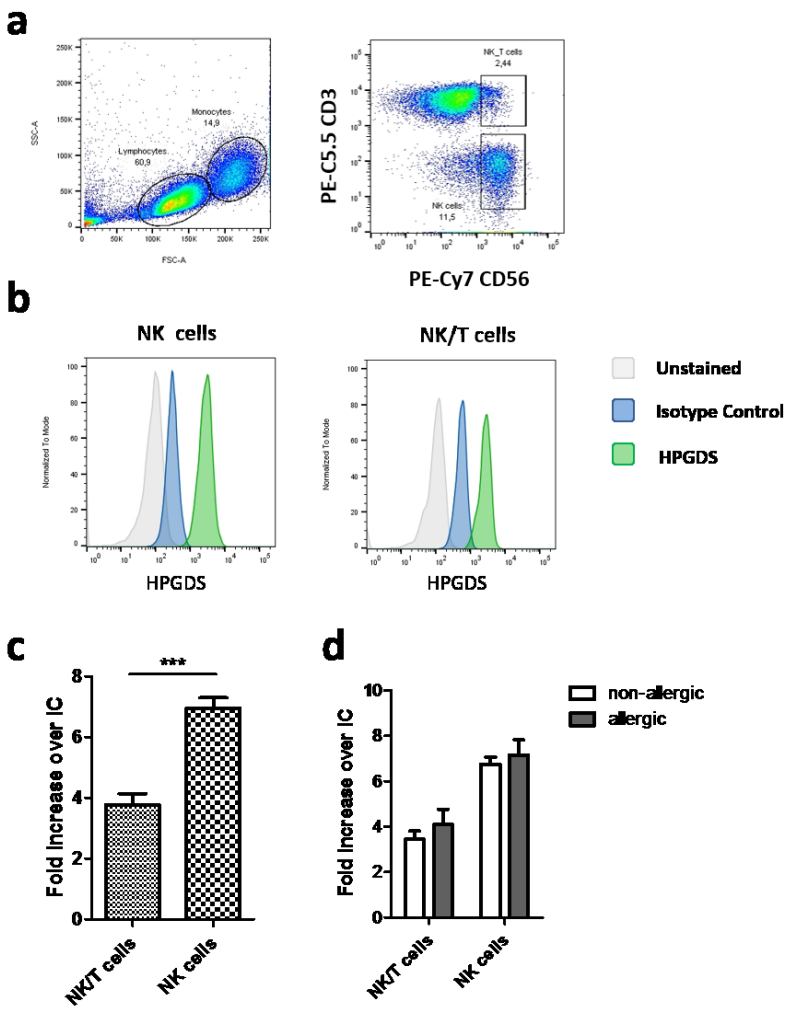

Figure 12. Circulating NK and NK/T cells express HPGDS. Flow cytometric analysis of HPGDS expression by immunostaining in PBMC fraction of peripheral blood. (a) Gating strategy for NK and NK/T cells. The lymphocyte region was selected and CD3/CD56 double positive NK/T cells and $CD3^{-}/CD56^{+}$ NK cells were picked for HPGDS expression analysis. (b) Representative graphs used for determination of HPGDS fold increase over IC. An almost total peak separation between HPGDS and IC signal can be observed for both populations. (c) NK-cells have a significantly higher HPGDS signal fold increase over IC. However, NK/T cells also show a distinct increase. (d) A tendency of increased expression, however, no significant difference in HPGDS expression between healthy and allergic donors could be identified. (n = 5, mean ± SEM, Two-way ANOVA with Bonferroni post-test, (*p<0.05, **p<0.01, ***p<0.001)

4.2.2 Circulating NK cells and the majority of NK/T cells potentially influence PGD_2 levels

NK and NK/T cells have the potential to tip the scale towards a pro-inflammatory environment, however, whether NK and NK/T cells participate in PGD_2 production still needs to be elucidated.

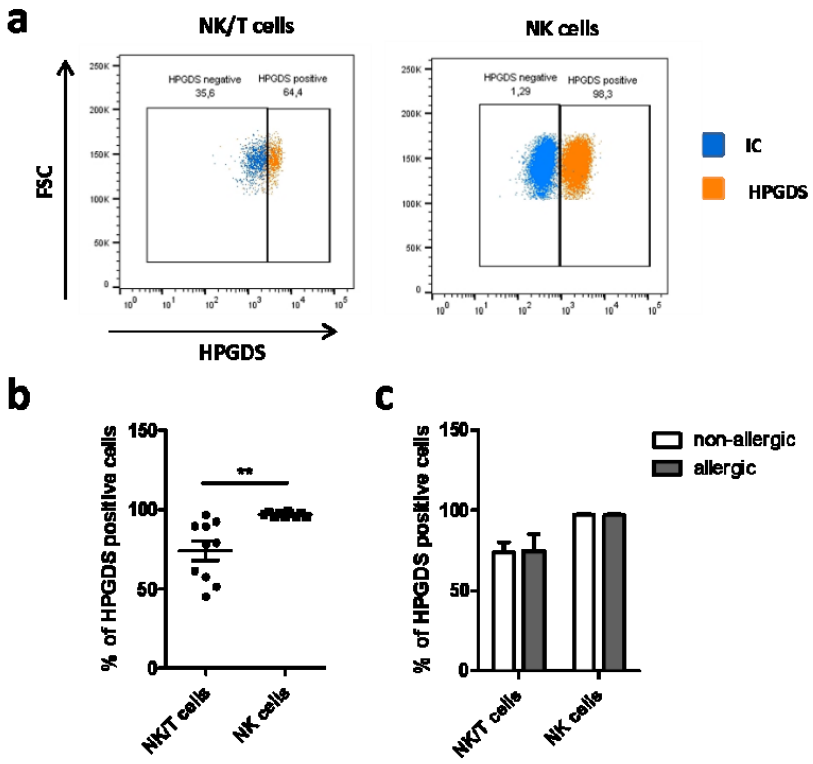

Figure 13. NK cells and the majority of NK/T cells are HPGDS positive. Flow cytometric analysis of HPGDS expression by immunostaining in PBMC fraction of peripheral blood. (a) Representative images of IC and HPGDS stained NK and NK/T cell populations. An almost perfect separation can be seen for NK cells. (b) HPGDS expression is significantly ($p<0.0011$) lower in NK/T cells, however, still the majority (74 %) were HPGDS positive. (n = 10, mean ± SEM, student t-test, $^{**}p<0.01$) (c) No difference in HPGDS expression could be observed between allergic and healthy donors. (n = 5, mean ± SEM, Two-way ANOVA with Bonferroni post-test, ($^{*}p<0.05$, $^{**}p<0.01$, $^{***}p<0.001$)

We identified circulating NK and NK/T cells by surface marker expression in PBMC fraction of peripheral blood, whereby NK cells were characterized as $CD3^{-}/CD56^{+}$ and NK/T cells as $CD3^{+}/CD56^{+}$ (Figure 12a). Both cell types show a high expression of HPGDS as seen by the flow-cytometric histograms (Figure 12b), which is even more pronounced in the NK cell population as compared to NK/T cells with a 6.9 and 3.8 -fold increase, respectively. No significant difference in HPGDS expression between allergic and control subjects could be observed (Figure 12d). Analyzing the percentage of HPGDS positive cells showed a clear separation as almost the entire NK cell population (97 %) as well as the majority of NK/T cells (74.1 %) stained positive (Figure 13a and b). While there was a significant difference in expression between NK and NK/T cells (Figure 13b), there was no difference between allergic and control subjects in either cell type (Figure 13c).

4.2.3 Peripheral blood neutrophils and eosinophils express low levels of HPGDS

Since both eosinophils and neutrophils are involved in pulmonary inflammatory reactions with elevated PGD_2 levels, here we investigated HPGDS expression in granulocytes to evaluate their potential participation in elevating PGD_2 levels.

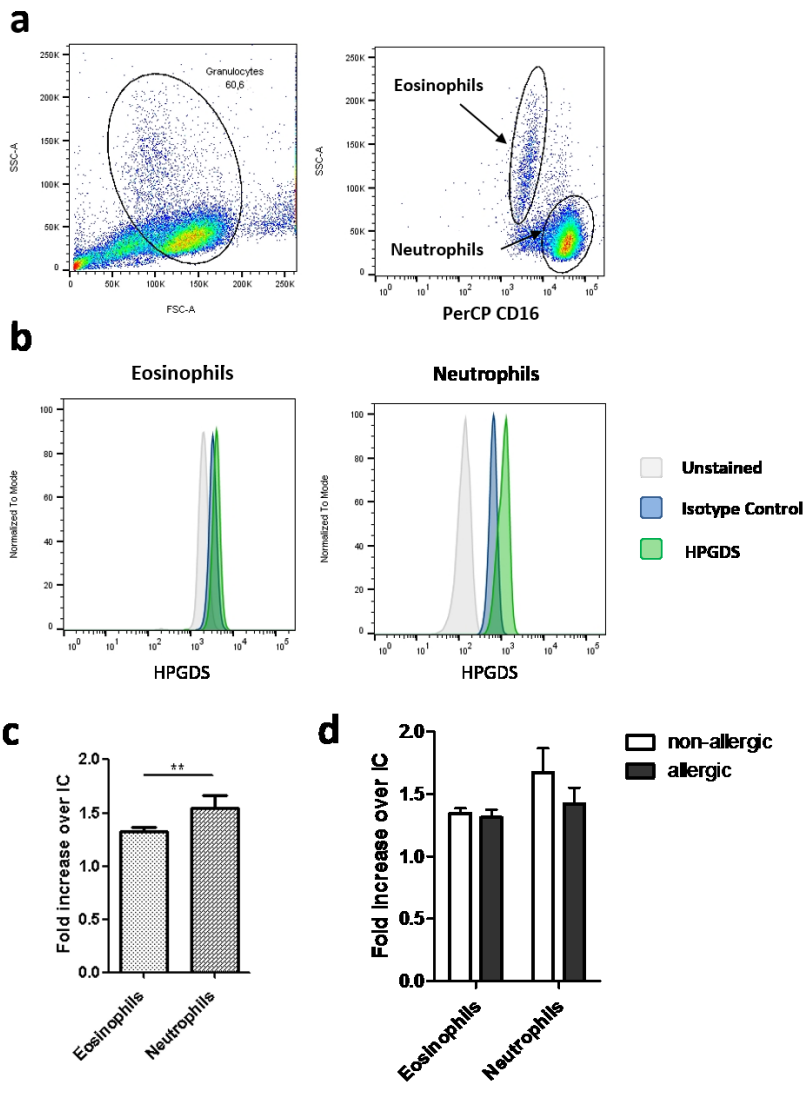

Figure 14. Peripheral blood neutrophils and eosinophils express low levels of HPGDS. Flow cytometric analysis of HPGDS expression by immunostaining in PMNL fraction of peripheral blood. (a) Gating strategy for neutrophils and eosinophils. Granulocyte region of PMNL was selected and $CD16^+$ neutrophils with low SSC as well as $CD16^-$ eosinophils with high SSC were picked. (b) Representative graphs of IC vs HPGDS signal in the AF488 channel. (c) Neutrophils have a significantly higher HPGDS fold increase over IC ($p<0.01$). (n = 10, mean ± SEM, Student's t-test, $^{**}p<0.01$) (d) In non-allergic subjects, there is a tendency of higher HPGDS expression in neutrophils and no difference in eosinophils. (n = 5, mean ± SEM, Two-way ANOVA with Bonferroni post-test, ($^*p<0.05$, $^{**}p<0.01$, $^{***}p<0.001$)

Eosinophils and neutrophils were analysed in the polymorphonuclear leukocyte (PMNL) fraction of peripheral blood, which contains mostly granulocytes. CD16 positive neutrophils were selected and CD16 negative eosinophils with characteristically high SSC (Figure 14a). Both, eosinophils and neutrophils showed a very low fold increase over IC, 1.3 and 1.5, respectively, indicating HPGDS expression at very low levels (Figure 14c). Additionally, there was no difference in HPGDS fold increase over IC between allergic and non-allergic donors in eosinophils. In neutrophils, however, there seems to be a tendency

of a higher HPGDS expression in non-allergic subjects (Figure 14d). Moreover, no distinct HPGDS positive populations could be detected neither in eosinophils nor in neutrophils – representative images are shown in Figure 15a.

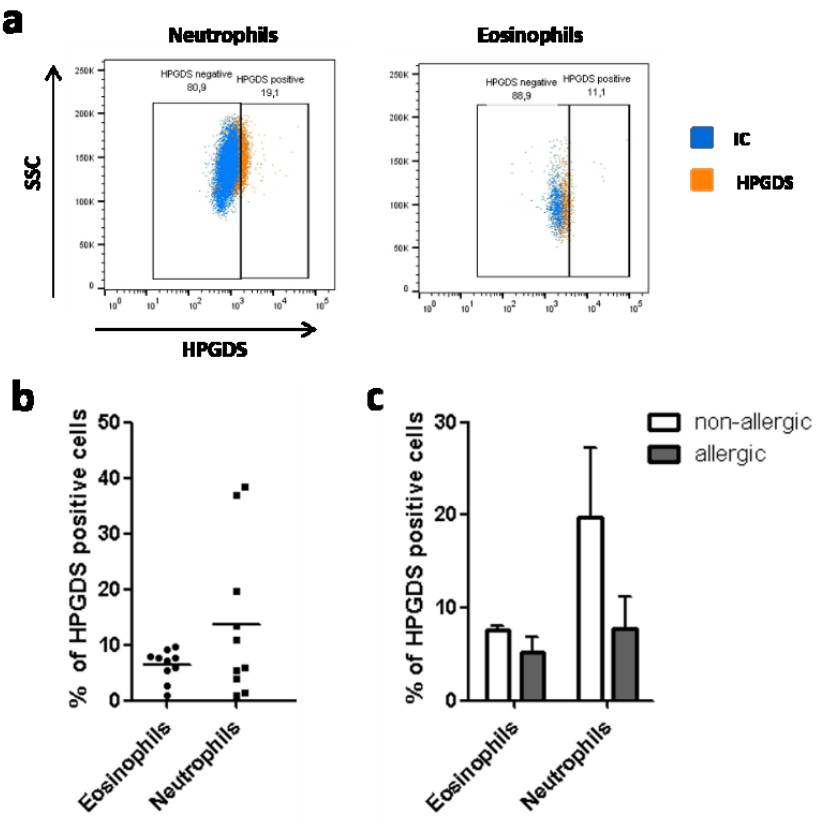

Figure 15 No distinct HPGDS positive population can be found in circulating neutrophils and eosinophils. Flow cytometric analysis of HPGDS expression by immunostaining in PMNL fraction of peripheral blood. (a) Both, eosinophil and neutrophil populations show a slight signal increase in the AF-488 channel. (b) A low percentage of eosinophils are HPGDS positive, however, a greater variation could be seen in neutrophils ranging from 2 – 40 % positive cells. (n = 10, mean ± SEM, Student t-test, n.s.) (c) In allergic subjects, a higher percentage of neutrophils were HPGDS positive, although, a great variation was seen. Also in eosinophils this tendency was visible. (n = 5, mean ± SEM, Two-way ANOVA with Bonferroni post-test, *p<0.05, **p<0.01, ***p<0.001)

Still, 6.4 % of eosinophils and 13.7 % of neutrophils stained positive for HPGDS when setting the threshold according to the corresponding IC signal. Interestingly, 19.7 % of neutrophils from non-allergic donors were HPGDS positive as compared to only 7.7 % of neutrophils in allergic donors (Figure 15c). Due to the great variation this result was not significant. The same tendency was observed in eosinophils, however, at a lesser extent.

4.2.4 B cells and Plasma cells

Plasma cells rather than B cells have been associated with actively influencing their environment by secretion of mediators. Here we evaluated HPGDS expression in both cell types.

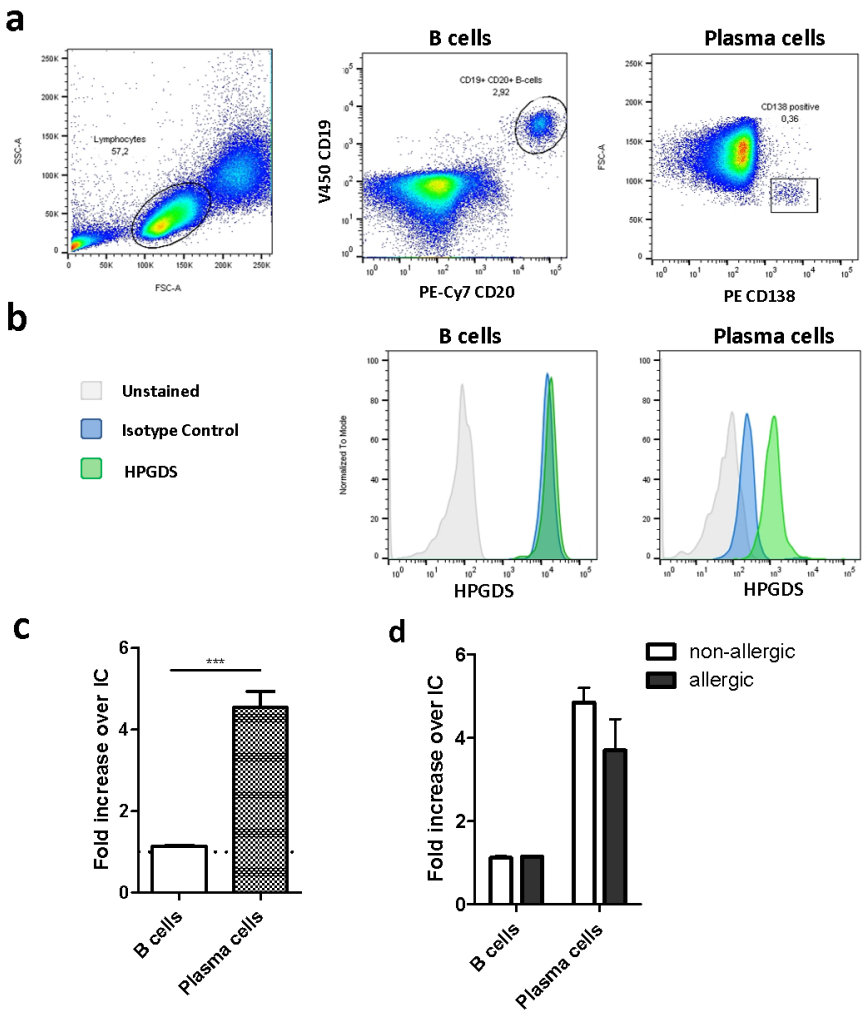

Figure 16. Differential expression of HPGDS in B and plasma cells. To determine HPGDS expression in B and plasma cells by flow cytometry, the PBMC fraction of peripheral blood was directly labelled: (a) CD19 and CD20 double positive B cells in the lymphocyte gate were selected for analysis. Further, the CD138 positive plasma cell population with low FSC was selected. (b) Representative images for HPGDS fold increase over IC. (c) HPGDS is upregulated during B cell activation to plasma cells. (B-cells n = 8, plasma cells n = 6; mean ± SEM, Student t-test $p < 0.001$). (d) In allergic subjects, plasma cells showed a tendency of less HPGDS expression, while there cannot be seen a difference in B cells. (B cells n = 3 (allergic) and n = 5 (non-allergic), plasma cells n = 3; mean ± SEM)

We selected CD19 and CD20 double positive B cells and CD138 positive plasma cells from the lymphocyte gate of PBMCs (Figure 16a), whereby numbers of circulating $CD138^+$ plasma cells were quite low in all donors. As with the other leukocyte subsets, here we also

calculated the HPGDS fold increase over IC with graphs representative for donors shown in Figure 16b.

In B cells, a HPGDS fold increase over IC was non-existent, while HPGDS expression seems to be upregulated after plasma cell differentiation. In plasma cells a 4.2-fold increase over IC could be observed, which is in comparison to B cells significantly higher (Figure 16c). In plasma cells, there was a tendency of less HPGDS expression in allergic donors when looking at fold increase over IC, while in B cells no difference was visible (Figure16d). Further, the majority of plasma cells (71 %) were HPGDS positive while no positive population was observed in B cells (Figure 17a and b). Here, no difference between allergic and non-allergic donors could be seen in both populations (Figure 17c).

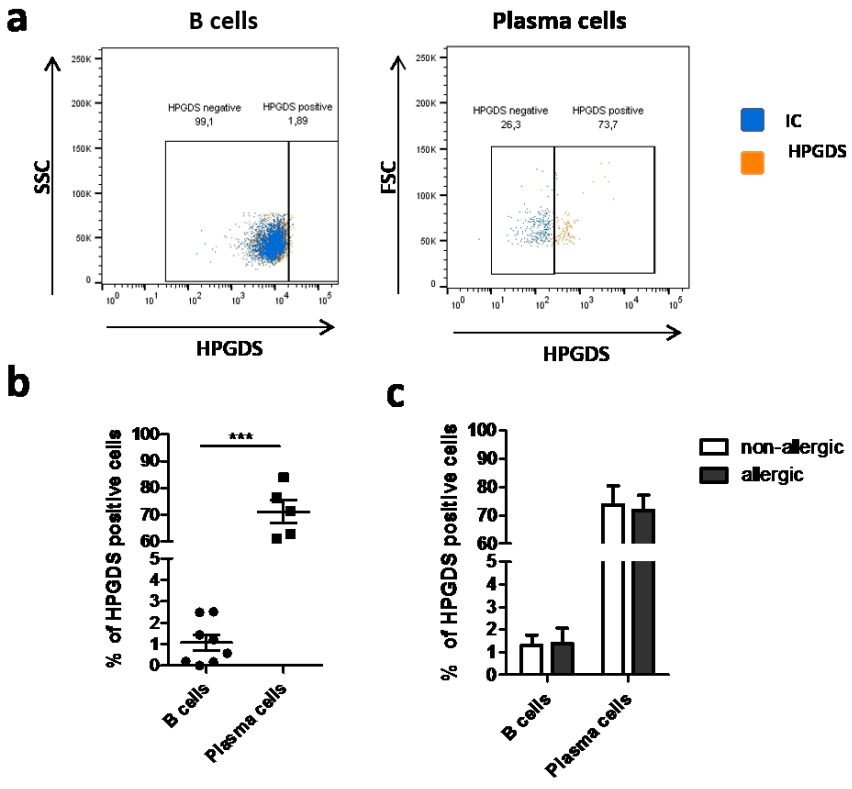

Figure 17. HPGDS ssion is ulated during B maturation to plasma cells. percentage of S positive cells evaluated with IC stained cells as nce. (a) Hardly any e B cells can be ed, however, a e population can en in plasma cells. The majority of a cells was HPGDS e which was a ant increase in rison to B cells (B- = 8, plasma cells n mean ± SEM, t's t-test p < (c) No difference e percentage of S positive cells en allergic and non- donors could be observed for both populations. (B cells n = 3 (allergic) and n = 5 (non-allergic), plasma cells n = 3; mean ± SEM)

To sum up our screening for HPGDS expression in immune cells from human peripheral blood, the results obtained for each cell population were compared, including HPGDS fold increase over IC (Figure 18a) and percentage of HPGDS positive cells (Figure 18b).

Resting and IL-4-activated MDM (M2) clearly show the highest difference between IC and HPGDS signal, followed by MDM activated with LPS/INF-γ (M1). From the leukocyte subsets tested, NK cells showed the highest fold increase over IC, followed by plasma cells, NK/T cells and $CD4^+$ T-cells. In circulating monocytes, eosinophils, neutrophils, $CD8^+$ T-cells and B-cells, HPGDS expression could hardly be detected. To assess whether HPGDS is differentially expressed within the leukocyte subsets, we determined the percentage of HPGDS positive cells. Almost 100 % of human MDM, M1 and M2 macrophages as well as circulating NK cells were HPGDS positive. The majority (~70 %) of peripheral blood NK/T cells, $CD4^+$ T-cells and plasma cells were HPGDS positive, making them also potential sources of PGD_2 production under homeostatic or inflammatory conditions. About 20 % of $CD8^+$ T-cells and neutrophils stained positive as well, while only 7 % of eosinophils were HPGDS positive and hardly any monocytes or B-cells.

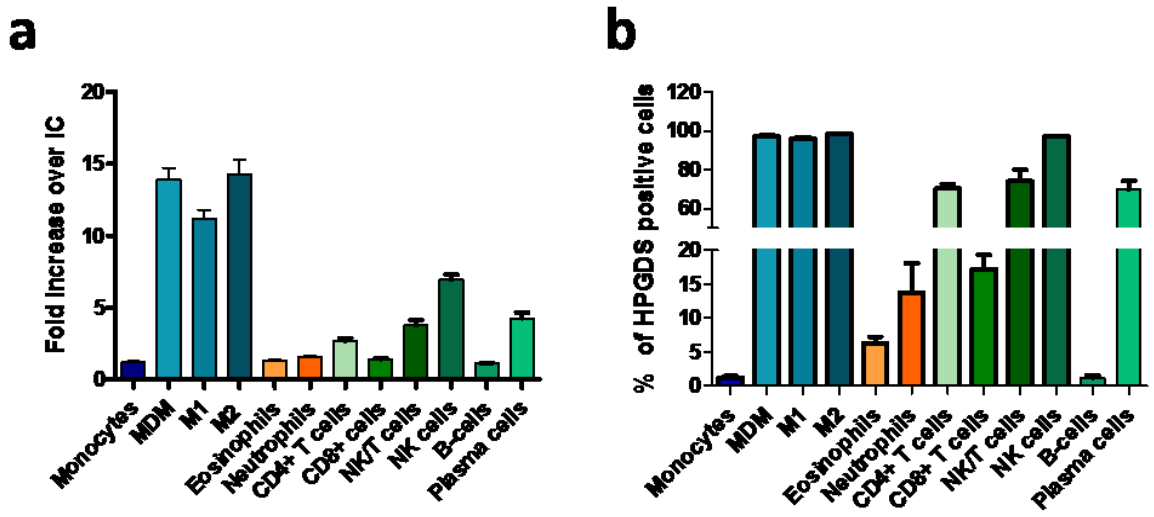

Figure 18. Differential HPGDS expression in homeostatic and activated MDM in comparison to circulating leukocyte subsets. HPGDS expression in immune cells was evaluated by indirect intracellular staining for the enzyme followed by flow cytometric analysis. (a) Geometric mean fold increase over IC for the cell types examined. MDM, M1 and M2 macrophages showed the highest difference between HPGDS and IC stained cells, while M1 macrophages had the least fold increase. NK cells had the highest fold increase over IC of all circulating leukocytes, followed by NK/T, plasma cells and $CD4^+$ T-cells. (b) The percentage of HPGDS positive cells was evaluated for all groups to identify different subsets within leukocytes. Almost 100 % of macrophages and NK cells were HPGDS positive as well as the majority (70 %) of NK/T cells, plasma cells and $CD4^+$ T-cells. About 15-20 % of neutrophils and $CD8^+$ T-cells and 7 % of eosinophils were HPGDS positive while hardly any monocytes and B-cells. (n = 10, B-cells (n = 8), plasma cells (n = 6); mean ± SEM)

4.3 PART III – LPS stimulates PGD_2 production in monocytes and macrophages most prominently

Finally, we set out to evaluate the amount of PGD_2 released by monocytes and macrophages under homeostatic and activated conditions. Additionally, alveolar macrophages from a mouse model of LPS-induced acute lung injury (ALI) and a mouse model of allergic asthma (OVA) were isolated and PGD_2 release compared.

4.3.1 LPS/INF-γ activation of human MDM triggers PGD_2 release *in vitro*

Previously, we could show that HPGDS is upregulated during macrophage differentiation *in vitro* and homeostatic MDM as well as M1 and M2 macrophages stained highly positive for HPGDS, the rate-limiting enzyme of PGD_2 production in cells of the hematopoietic lineage. Now we were interested in the PGD_2 production levels of macrophages under resting conditions and activated either with 100 ng/ml LPS and 20 ng/ml INF-γ or IL-4.

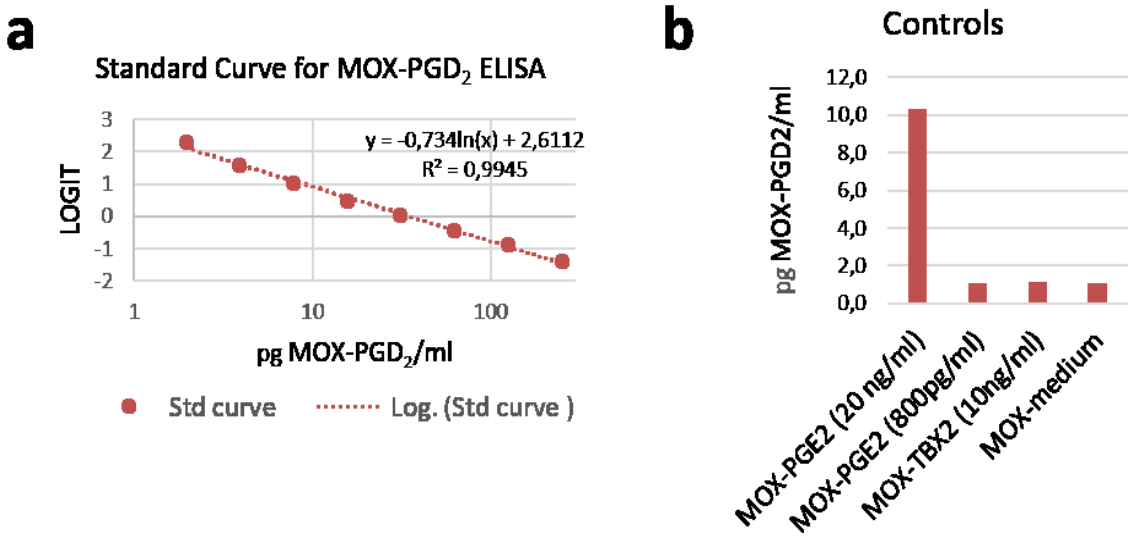

Figure 19. Standard curve and controls performed for MOX-PGD_2 ELISA. (a) Representative MOX-PGD_2 standard curve assayed in duplicate ranging from 2 – 250 pg MOX-PGD_2 /ml. MOX-PGD_2 concentrations were plotted against LOGIT values calculated from absorbance (A) at 410 nm (LOGIT = ln(A/(1-A)) to yield a linear standard curve. Obtained equation had an R^2 value of 99.45 % was used for the calculation of MOX-PGD_2 concentration in samples. (b) Controls were performed to estimate the extent of non-specific binding, i.e. cross-reaction of the antibody. 20 ng MOX-PGE_2/ml resulted in a signal of 10 pg MOX-PGD_2/ml (0.05 % cross-reactivity), while 800 pg MOX-PGE_2/ml, 10 ng MOX-TBX_2/ml and MOX-medium only resulted in values below the detection level (2 pg/ml).

Following activation, conditioned medium as well as protein lysates for normalization were collected after 4, 8, 24 and 48 hours. The amount of released PGD_2 was evaluated with a MOX-PGD_2 ELISA kit using a MOX-PGD_2 standard curve assayed for each plate. A representative standard curve obtained with the MOX-PGD_2 ELISA kit is shown in Figure 19a, whereby MOX-PGD_2 concentrations were plotted against LOGIT values calculated from absorbance (A) at 410 nm (LOGIT = ln(A/(1-A)) to yield a linear standard curve. To evaluate non-specific binding, MOX-PGE_2, MOX-TBX_2 and MOX-medium was measured, whereby 20 ng/ml MOX-PGE_2 resulted in a signal of 10 pg/ml MOX-PGD_2 (0.05 % cross-reactivity) and TBX_2 as well as medium resulted only in values below the detection level (Figure 19b).

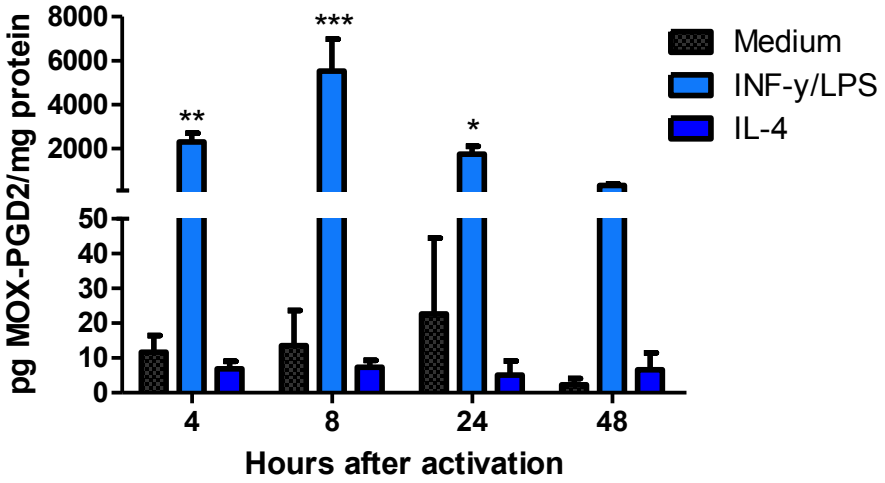

Figure 20. LPS/INF-γ stimulation of human MDM (M1) induces PGD_2 secretion *in vitro*. Peripheral blood monocytes were differentiated into human MDM, which in turn were left in resting state (MDM), activated with 100 ng/ml LPS and 20 ng/ml INF-γ (M1) or 20 ng/ml IL-4 (M2). Conditioned medium was collected at 4, 8, 24 and 48 h after activation and a methoximating reaction was performed to yield MOX-PGD_2. The amount of MOX-PGD_2 present in conditioned medium was evaluated with a MOX-PGD_2 ELISA kit (Caymen). Released MOX-PGD_2 produced by macrophages was normalized to total protein/well. 8 hours after activation LPS/INF-γ stimulation triggered most PGD_2 release (n = 6, mean ± SEM, Two-way ANOVA with Bonferroni post-test, (*p<0.05, **p<0.01, ***p<0.001)

Classically activated human MDM with LPS/INF-γ released most PGD_2 at all four time points, with peak PGD_2 release being observed after 8h. To exclude the influence of variations in the cell numbers in the wells, the amount of PGD_2 detected in 1 ml medium - released by approximately $1x10^6$ macrophages - was normalized to total protein content in the corresponding well (Figure 20). Levels of PGD_2 after 4 and 8 hours of activation with LPS/INF-γ-stimulation were as high as 2 ng PGD_2/mg protein and 6 ng PGD_2/mg protein, respectively. In contrast, medium only (MDM) and IL-4 stimulation (M2) did not result in

much PGD_2 secretion. The highest average amount of PGD_2 released by MDM was about 20 pg PGD_2/mg protein after 24 hours incubation.

4.3.2 Murine alveolar macrophages isolated after LPS-induced acute lung injury release most PGD_2

To evaluate PGD_2 production by macrophages in alveoli, we isolated alveolar macrophages by bronchoalveolar lavage from healthy mice as well as from mice with acute lung injury and allergic asthma. Isolated cells with BAL fluid were counted and, additionally, the number of alveolar macrophages was determined by morphology.

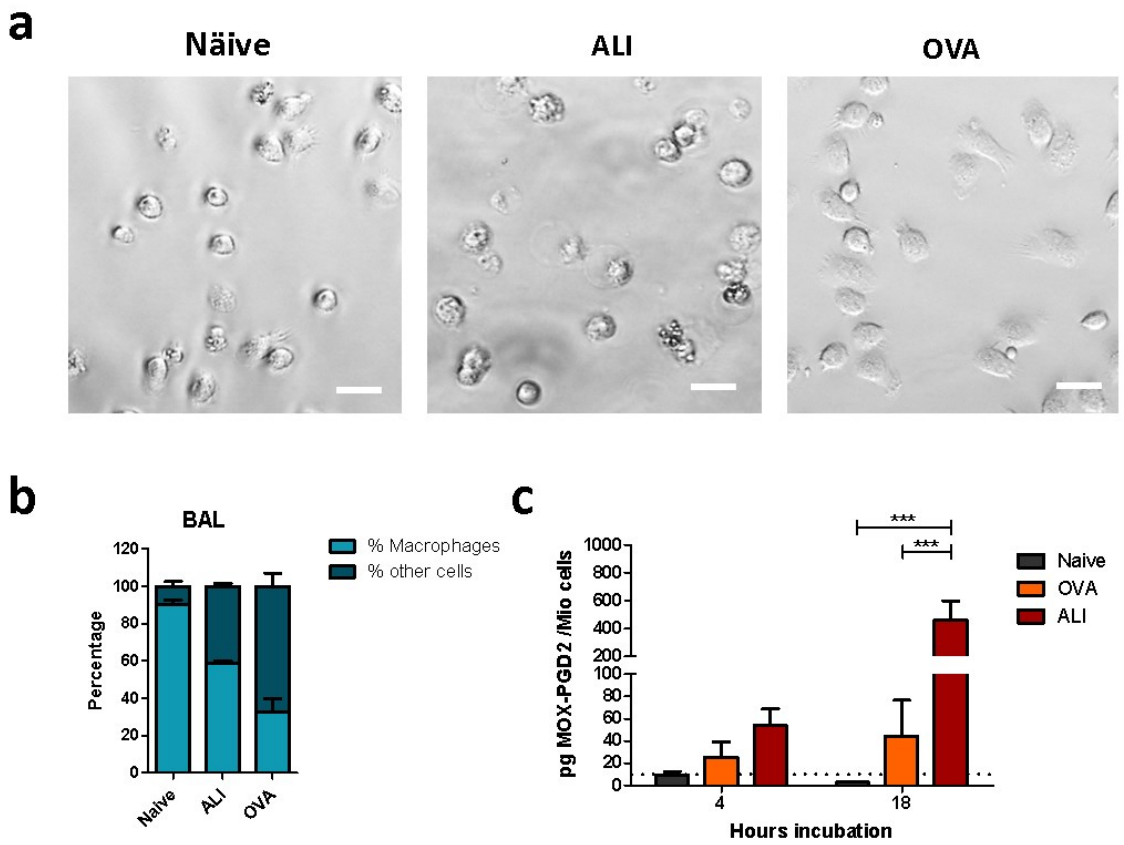

Figure 21. Murine alveolar macrophages from LPS-induced acute lung injury isolated with BAL produce significant levels of PGD_2 in vitro. Alveolar macrophages were isolated from ovalbumin (OVA) – sensitized asthmatic mice, mice subjected to LPS-induced acute lung injury (ALI) and naïve mice as control by broncho-alveolar lavage. Alveolar macrophages were counted and cultured at similar densities for 4 and 18 hours. Conditioned medium was methoximated and PGD_2 content was measured with a MOX-PGD_2 ELISA kit (Cayman). (a) Representative light microscopy images of mouse alveolar macrophages from the three different groups of mice – naïve, ALI and OVA. (scale bar 10 µm) (b) Cellular composition of BAL fluid. Alveolar macrophages were identified morphologically whereby naïve mice had the highest macrophage percentage and OVA mice the lowest (n = 5, mean ± SEM). (c) Amount of MOX-PGD_2 (pg/ Mio alveolar macrophages) in conditioned medium of naïve, OVA and ALI mice. Alveolar macrophages isolated from ALI mice produced significantly more PGD_2 than those from naïve and OVA mice. (n = 5, mean ± SEM, Two-way ANOVA with Bonferroni post-test, (*$p<0.05$, **$p<0.01$, ***$p<0.001$)

A high number of immune cells could be seen in ALI lungs with an average of 79 ± 24 Mio cells collected with BAL fluid, of which 0.346 ± 0,086 Mio were macrophages. With the BAL fluid of OVA mice an average of 1.27 ± 0.84 Mio cells (0.308 ± 0.012 Mio macrophages) could be obtained while in naïve mice only 0.224 ± 0.111 Mio cells were collected and the majority could be identified as alveolar macrophages (0.204 ± 0.108 Mio). In naïve mice, 90 % of cells in BAL fluid could be identified as macrophages, about 60 % in the allergic asthma model, while in acute lung injury only 33 % were macrophages (Figure 21b).
In Figure 21a light microscopy images are displayed of alveolar macrophages in culture isolated from naïve, ALI and OVA mice. There are small morphological differences between alveolar macrophages isolated from the three different groups; however, for all subjects a homogenous cell composition could be achieved by differential adhesion on CellBind plates.

Alveolar macrophages isolated from naïve mice produced hardly any detectable levels of PGD_2, while macrophages from OVA-mice produced low amounts but steadily and also increased levels after 18 h in culture. Macrophages from LPS-induced acute lung injury produced the highest amount of PGD_2 at all time points. However, the peak of PGD_2 production by ALI-alveolar macrophages was observed after 18 h of culture (~ 500 pg MOX-PGD_2/Mio alveolar macrophages) (Figure 21c).

4.3.3 Monocytes release PGD_2 upon LPS/INF-γ stimulation

Until now, PGD_2 production in monocyte has not been addressed in detail. We were interested is assessing whether monocytes produce PGD_2 under homeostatic or activated conditions, whereby we used the same conditions, including stimulants and time points, as previously described for macrophages. Monocytes were incubated with activation medium including stimulants and conditioned medium was collected 4, 8, 24 and 48 hours after activation.
PGD_2 levels in each well were normalized to total cellular protein to balance minor alterations in cell number in each well. Results indicate that at the 24 h time point most PGD_2 was secreted by monocytes that have been stimulated with LPS/INF-γ (36 ng PGD_2/mg protein) (Figure 22). Also at the other time points, a significant difference was detectable between LPS/INF-γ stimulation and medium only or IL-4 treatment. Monocytes incubated with medium only released approximately 1.1 ng PGD_2/mg protein after 8 hours of incubation and IL-4-stimulated monocytes even less.

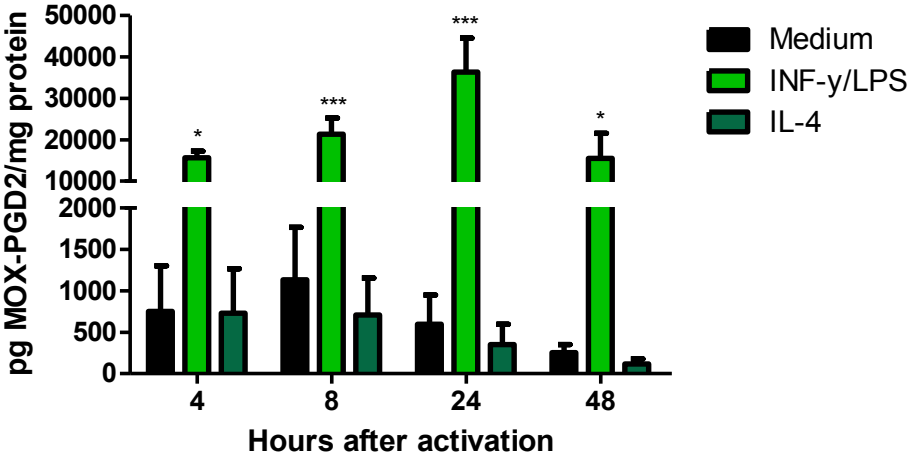

Figure 22. LPS stimulation potentiates PGD_2 release by monocytes. Peripheral blood monocytes were isolated from PBMC using differential adhesion and, subsequently, cells were incubated with activation medium, medium with 20 ng/ml INF-y and 100 ng/ml LPS or 20 ng/ml IL-4 and the conditioned medium was collected at 4 time points. LPS-stimulation triggered PGD_2 release most potently at all 4 time points. Medium only and IL-4 resulted in less PGD_2 release, while IL-4-treated monocytes resulted in even less PGD_2 secretion. Amount of PGD_2 released by monocytes was normalized to total amount of protein/well. (n = 3, mean ± SEM; Two-way ANOVA with Bonferroni post-test, *p<0.05, **p<0.01, ***p<0.001)

4.3.4 LPS/INF-γ-stimulated monocytes released more PGD_2 than MDM at all four time points

A comparison of PGD_2 secreted by LPS-stimulated monocytes and MDM at all four time points is displayed in Figure 23. Human monocytes released higher levels of PGD_2 after LPS-stimulation than human MDM *in vitro*, which sheds new light on the role of monocytes in acute lung injury. Looking at protein-normalized values, there is a striking difference in detected PGD_2 levels. PGD_2 release after LPS activation peaks after 8 hours in MDM but, after 24 hours in monocytes. At all four time points monocytes produced significantly more PGD_2 than MDM. The rapid onset of PGD_2 production in monocytes suggests a quick response after activation with LPS while production declines again between 24 and 48 hours. In MDM, PGD_2 production already drops after 8 hours of activation, showing a short-term increase in prostanoid production compared to monocytes.

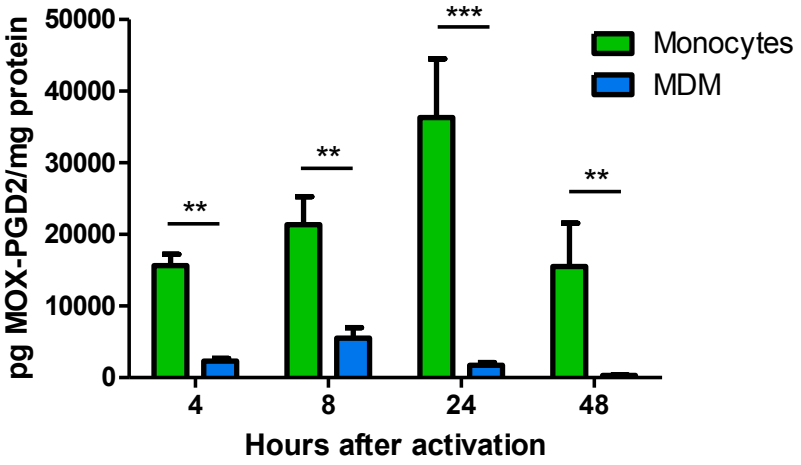

Figure 23. Comparison of PGD_2 secretion of LPS-stimulated monocytes and MDM. Conditioned medium from monocytes or monocyte-derived macrophages (MDM) was collected 4, 8, 24 and 48 hours after activation with INF-γ/LPS and secreted PGD_2 was measured. Comparison of pg PGD_2/mg protein released by monocytes (green) or MDM (blue) after stimulation. Secreted PGD_2/ml was normalized to mg cellular protein per well for monocytes an MDM stimulated with INF-γ/LPS. Monocytes produced significantly more PGD_2 with maximum levels found 24 h after activation. (monocytes n = 3, MDM n = 6; mean ± SEM; Two-way ANOVA with Bonferroni post-test, *p<0.05, **p<0.01, ***p<0.001)

4.4 PART IV - PGD_2 stimulation of human MDM diminishes pro-angiogenic effect of homeostatic macrophages in CAM assay

Previous studies have shown that PGD_2 activation of DP1 and DP2 receptors on human MDM results in pro-inflammatory effects in the lung [2]. Additionally, in macrophages a pro-inflammatory phenotype mostly goes along with anti-angiogenic properties, while the anti-inflammatory M2 macrophages are associated with promoting neovascularization. Angiogenesis under homeostatic conditions is crucial to facilitate proper lung function, however, in pulmonary disorders including lung fibrosis, primary and metastatic cancers and in the fibro-proliferative stages of ARDS, these mechanisms are disordered and heterogeneous [3]. We were interested in whether resting human MDM and PGD_2-activated MDM influence angiogenesis and to which extent. Therefore, we performed preliminary experiments using the chicken chorioallantoic membrane (CAM) assay to evaluate angiogenic effects of macrophage - conditioned medium on neovascularization. To this end, MDM were stimulated 4 times within 48 hours with either vehicle (EtOH), 300 nM PGD_2 or 1 µM PGD_2, then the medium was changed and conditioned medium was collected 6 h later.

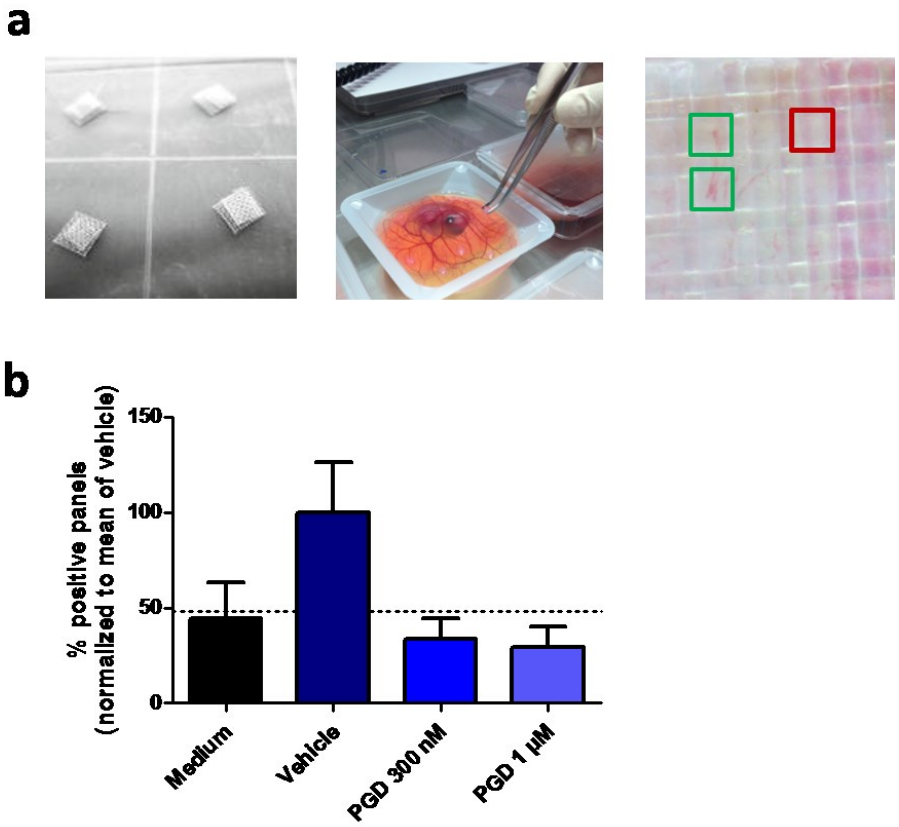

Figure 24. PGD_2 treatment of MDM prevents their pro-angiogenic effect. Monocyte-derived macrophages were treated with 1 µM and 300 nM PGD_2 or with PGD_2 vehicle. Conditioned medium containing no exogenous PGD_2 was collected and its angiogenic properties assessed with a CAM assay. (a) Nylon grid sandwiches were used to allow polymerization of collagen-containing onplant mixture. These onplants were layered on the CAM of 10-day-old chicken embryos and incubated for 3 days at 37 °C. Positive and negative panels were counted, panels considered positive or negative are indicated with green or red squares, respectively. (b) Results from 3 independent experiments were normalized to the mean of vehicle. Vehicle treated MDM have a pro-angiogenic effect in CAM (n = 8), which is diminished by PGD_2 treatment (n = 5). Medium only as negative control resulted in 50 % fewer positive panels (n = 2). (mean ± SEM; One-way ANOVA, n.s.)

Conditioned medium from 4 donors was pooled, mixed with a collagen-containing master-mix and transferred to previously assembled nylon grid sandwiches (Figure 24a). After polymerization, onplants were placed onto the CAM of 10-day-old chicken embryos and sprouting of newly formed vessels into the space between the two nylon grids was evaluated by counting positive and negative panels after 72 h incubation (Figure 24a). The percentage of positive panels was determined for all conditions and the results from 3 experiments were normalized to the mean of vehicle and are displayed in Figure 24b. Panels with culturing medium only showed about 50 % fewer positive panels than vehicle treated MDM (100 %). Treatment of MDM with 300 nM PGD_2 resulted in 36 % positive panels and 1 µM PGD_2 in 33 % positive panels. Both concentrations of PGD_2 resulted in reduction of angiogenesis in comparison to vehicle-treated MDM, indicating a suppression of angiogenic potential through macrophages that have been activated with PGD_2. However, further experiments will be conducted to confirm these preliminary data.

5 Discussion

In the lung, PGD_2 has mostly been linked to allergic diseases as it is released by activated mast cells, thereby inducing vasodilation and inflammation [4]. Recently, elevated PGD_2 levels were detected in a LPS-induced mouse model of acute lung injury, which closely relies on macrophages orchestrating the immune response and involves hardly any mast cells [2]. Therefore, the major interest of this study lies on shedding more light on PGD_2 production by human monocytes and macrophages under homeostatic and activated conditions. This is achieved on the one hand by characterizing the differential expression of HPGDS on a variety of leukocyte subsets, and on the other hand by directly measuring PGD_2 secretion *in vitro*. Other immune cells were investigated as potential PGD_2 sources by evaluating HPGDS expression by flow cytometry. Additionally, we isolated alveolar macrophages from murine models of acute lung injury and allergic asthma to evaluate PGD_2 secretion by macrophages in pulmonary inflammation. Zhao et. al. could already show that murine bone marrow-derived macrophages express HPGDS and are able to produce and release PGD_2 upon LPS stimulation [5]. Now we wanted to evaluate HPGDS expression and PGD_2 production by human monocytes and macrophages.

Here we could show that circulating human monocytes express hardly any HPGDS on protein and mRNA level, whereby there was no difference between allergic and non-allergic donors. However, *in vitro* differentiation of peripheral blood monocytes into monocyte-derived macrophages resulted in an upregulation of HPGDS expression. A significant increase of HPGDS expression could be determined in homeostatic MDM as well as activated M1 and M2 macrophages on protein level. These results indicate a selective upregulation of HPGDS expression during macrophage differentiation *in vitro*. In patients with inflammatory arthritis, a low HPGDS expression could be determined in peripheral blood monocytes; however, a slight upregulation seems to take place in synovial fluid monocytes while synovial fluid dendritic cells expressed significantly more HPGDS [6], which strengthens the hypothesis of an ongoing upregulation of HPGDS expression during monocyte differentiation. We could not see a difference in HPGDS expression between allergic and non-allergic donors, but post-translational modifications might pose a way to differentially regulate HPGDS function and PGD_2 production, though, none have been investigated yet.

On mRNA level, there was no difference in HPGDS expression between monocytes and M1 macrophages after 48 h of activation, while significantly more HPGDS mRNA was present in resting MDM and M2 macrophages. Whether HPGDS mRNA transcription can be reduced by negative feedback mechanisms is not known so far. Indeed, it would be

interesting to see whether mRNA levels change throughout the time course of M1 polarization.

Next we measured PGD_2 release by homeostatic and activated human monocytes and monocyte-derived macrophages as well as isolated murine alveolar macrophages from a LPS-induced mouse model of acute lung injury and a model of allergic asthma induced through OVA-challenge. LPS is a highly potent stimulator of monocytes and macrophages and strongly activates a pro-inflammatory reaction, which has mostly been associated with the vast secretion of PGE_2 [7]. Recently, it was shown that murine bone marrow-derived macrophages (BMDM) release high levels of PGD_2 after LPS-stimulation *in vitro* [5], although monocytes have not been primarily linked to elevated PGD_2 levels to date. Using a MOX-PGD_2 ELISA, we could show that LPS-activated human MDM released significantly higher amounts of PGD_2 than non-stimulated or IL-4 stimulated MDM at 4 and 8 hours after activation. This was interesting, as we found the lowest level of HPGDS expression in M1 macrophages on protein level and hardly any on mRNA level. However, we were looking at HPGDS expression 48 hours after activation and in the time course of PGD_2 production of human MDM the production level dropped already between 8 and 24 hours so there might be a negative feedback loop responsible for downregulation of HPGDS in M1 macrophages.

Also murine alveolar macrophages from LPS-induced lung injury produced significantly higher amounts of PGD_2 than alveolar macrophages isolated form the allergic mouse model and naïve mice. This suggests an important role of macrophages in elevated PGD_2 levels in acute lung injury. Detected PGD_2 levels were lower than shown by Zhao et. al. for murine BMDM, however, they used a 10-times higher LPS concentration for stimulation.

Interestingly, human monocytes released tremendous amounts of PGD_2 upon LPS stimulation, with most release after 8 and 24 h incubation. Therefore, the peak of PGD_2 release occurred later in monocytes than macrophages, whereby, monocytes released significantly more PGD_2 at all 4 time points. These high amounts of PGD_2 release came unexpected after obtaining the results for HPGDS expression in peripheral blood monocytes. We could hardly detect any HPGDS in non-activated circulating monocytes on protein and mRNA level; however, HPGDS expression might be upregulated upon activation, which needs to be further investigated. After LPS-stimulation COX-2 is induced and vast amounts of PGH_2 are produced by monocytes. Another possibility for PGD_2 production independent from HPGDS would be conversion of PGH_2 to PGD_2 by non-enzymatic pathways, which happens under certain conditions [8]. A rate-limiting role of HPGDS in human monocytes and MDM in PGD_2 production will need further investigation including selective pharmacological inhibition of COX and HPGDS and subsequent

evaluation of PGD_2 secretion. Additionally, COX inhibition in combination with providing PGH_2 will show whether HPGDS is the rate-limiting enzyme of PGD_2 production in human macrophages and monocytes. Although HPGDS has been shown to be the rate-limiting enzyme in PGD_2 production in murine BMDB and neither blocking COX-2 nor LPGDS influenced secreted PGD_2 levels [5], we cannot exclude that there might be other LPS-triggered downstream signalling events involved in increased PGD_2 production. In contrast, Joo et. al. claim that LPS can induce LPGDS in macrophages, which they could show to be important for PGD_2 production [9]. It seems to be controversial, which PGD synthase is responsible for PGD_2 production in macrophages. One crucial by-product of LPS stimulation of macrophages and monocytes is the production of ROS. It has been shown that the functional activity of HPGDS is closely linked to the presence of ROS in the cells, which suggests that introduction of ROS is necessary for PGD_2 production [5]. Besides ROS, HPGDS function is dependent on GST as co-factor, therefore, balanced NADPH/NADP levels play an important role in facilitating PGD_2 production.

In addition to monocytes and macrophages, a flow cytometric approach was chosen to investigate HPGDS expression in other circulating leukocyte populations, which have the ability to migrate through the vascular barrier into sites of inflammation upon activation through chemokines. Elevated PGD_2 levels could be detected in an LPS-induced mouse model of acute lung injury 4 hours after administration and we wanted to elucidate potential other PGD_2 sources next to monocytes and macrophages. Pulmonary inflammation can be grouped into type-1 or type-2 reactions depending on major cell types and cytokines involved. While the first is associated with elevated INF-γ and TNF levels and neutrophil infiltration, the latter is primarily characterized by IL-4, IL-5 and IL-13 secretion and eosinophil infiltration of the lung [10]. This categorization points to an important role of $CD4^+$ T-cells in shaping the immune response in pulmonary disorders. Here we could show that the majority of $CD4^+$ T-cells were positive for HPGDS, which goes along with previous findings about differential PGD_2 production by Th2 cells, a subset of $CD4^+$ T-cells [11]. Elevated PGD_2 levels in allergic asthma have mostly been associated with release from activated mast cells after antigen crosslinking of IgE-receptors [12]; however, our HPGDS screening showed a higher number of HPGDS positive $CD4^+$ T-cells in allergic donors, which indicates a potentially greater involvement of these cells in PGD_2 production in allergic asthma than estimated to-date. On the other hand, only a minor part of circulating $CD8^+$ T-cells, which are mostly responsible for specific cytotoxic reactions towards microorganisms, expressed HPGDS. Besides cytotoxic properties $CD8^+$ lymphocytes seem to be involved in inflammatory cell recruitment and tissue damage in COPD caused by cigarette smoke [13]. Until now, $CD8^+$ T-cells have not been considered as prostanoid-

producing cells, which makes a potent involvement in elevated PGD_2 levels unlikely. However, it would be interesting to see whether HPGDS expression is increased by activating stimuli since a certain percentage of $CD8^+$ T lymphocytes are positive.

Next, we looked at HPGDS expression in NK and NK/T cells by flow cytometry. NK cells are cytotoxic cells that have been shown to influence immune-pathological processes mostly by secretion of INF-γ and TNF-α [14], thereby, shifting the inflammatory response towards a type-1 response. Indeed, it has been shown that PGD_2 suppresses NK cell function through DP receptor activation, including pro-inflammatory mediator secretion, which promotes a type-2 immune response typical in allergic diseases [15,16]. Prostanoid production by NK cells has not deemed likely so far, thus, a striking finding of this HPGDS screening was that NK cells seem to express HPGDS constitutively and as close to 100 % of cells stained positive. Certainly, no functional conclusion can be drawn from this preliminary screening, but due to this distinct result NK cells might be a potential source of PGD_2. In addition, the majority of NK/T cells stained positive for HPGDS in this screening. While NK/T cells share most of their functional characteristics with NK cells, they additionally possess a T-cell receptor, which facilitates antigen-specific activation and targeted cytotoxic reactions. PGD_2 has also been reported to suppress INF-γ secretion by NK/T cells [17], however, like NK cells, NK/T cells have not been considered as potential prostanoid sources.

Granulocytes produce and release great amounts of inflammatory mediators, of which the majority are interleukins. Neutrophil infiltration is typical for a type-1 inflammatory reaction including acute lung injury, while eosinophil infiltration primarily happens in allergic reactions or defence mechanisms against parasites. Recently, Feng et. al. showed that $CD34^+$-derived eosinophils from patients with aspirin-exacerbated respiratory disease (AERD) express HPGDS and produce PGD_2 [18]. In this HPGDS screening, we found that 10 % of circulating, non-activated eosinophils express HPDGS, while there seems to be a tendency of fewer HPGDS positive eosinophils in allergic donors. This low number of positive eosinophils might be due to the non-activated state in peripheral blood and HPGDS expression is very likely to be upregulated upon activation or in certain disorders like AERD. In contrast to eosinophils, neutrophils have not been associated with PGD_2 production but rather produce PGE_2 and leukotriene B_4 (LTB_4) as well as vast amounts of ROS species besides releasing cytokines [19,20]. Here we could detect low HPGDS expression in peripheral blood neutrophils and, interestingly, neutrophils isolated from allergic donors tend to express less HPGDS than neutrophils from non-allergic donors. However, peripheral blood neutrophils stained significantly more positive for HPGDS than

eosinophils, which have already been shown to produce PGD_2 in AERD. But again, HPGDS expression might vary in different disorders and upon activation, and in this study the aforementioned cell types were investigated under resting conditions.

B cells and their effector cells termed plasma cells are primarily responsible for the humoral immune response by secretion of antigen-specific antibodies. Plasma cells, which circulate in small numbers in peripheral blood until they encounter a specific antigen, are also able to secrete inflammatory mediators [21]. We could not identify HPGDS expression in B-cells, but during B-cell differentiation to plasma cells HPGDS seems to be upregulated as the majority of plasma cells stained positive for HPGDS. Whether plasma cells secrete PGD_2 and under which conditions still remains to be investigated.

Besides deciphering origins of elevated PGD_2 levels in pulmonary disorders, we are specifically interested in the effect of PGD_2 on lung pathology next to immune modulatory functions. Ongoing and chronic inflammation results in tremendous tissue damage and functional impairment. Neovascularization in the lung needs to be tightly regulated as it is essential for efficient respiratory function and a dysregulation in angiogenesis is associated with pulmonary disorders [22]. Macrophages are key players in orchestrating various immunological reactions in the lung, which makes them an interesting target for further investigation. Jandl et. al. could show that activated PGD_2 receptors on macrophages results in aggravated neutrophil infiltration into the lung, thereby exerting a pro-inflammatory effect. In macrophages, a pro-inflammatory phenotype mostly goes along with anti-angiogenic properties and vice versa. Tumor-associated macrophages are primarily alternatively-activated and secrete pro-angiogenic factors including VEGF, IL-17 and IL-23 while classically activated macrophages have the opposite effect [23].
It has not been investigated to-date, whether activated DP1 and DP2 receptors on macrophages influence angiogenesis through release of mediating factors. So this was a novel approach to elucidate differential functionalities of PGD_2-activated macrophages. To assess pro- or anti-angiogenic effects, we decided to use a chicken chorioallantoic membrane (CAM) assay, which uses the CAM of 10-day-old chicken embryos that is still in development at this time point. The CAM is the respiratory tissue of chicken embryos during early development, which allows gas exchange through the egg shell, and due to ongoing neovascularization offers a great model for investigating angiogenesis [24]. We stimulated fully differentiated human macrophages with two different concentrations of PGD_2, changed the medium and applied macrophage-conditioned medium in collagen onplants on the CAM of chicken embryos. After 72 hours of incubation, a clearly visible difference between vehicle-treated and PGD_2-treated MDM was observed as more newly

sprouting vessels grew into the layer between nylon grids from vehicle-treated macrophages. This indicates the presence of pro-angiogenic factors, while these factors seem to be missing in conditioned medium from PGD_2-treated macrophages.
As mentioned earlier, inflammatory and angiogenic properties of macrophages are indirectly related, which indicates that homeostatic MDM that have been generated from monocytes by stimulation with M-CSF resemble the alternatively activated macrophages more closely. They also express mannose receptor (CD206), a surface marker for anti-inflammatory macrophages, however, at a lower level than M2 macrophages. With this preliminary experiment we could show, that PGD_2-treatment diminishes the pro-angiogenic effect. However, the responsible factor(s) for these effects still need to be discovered, whereby potential candidates would be M2 macrophage-associated pro-angiogenic factors like IL-17, IL-23 or even VEGF. Additionally, PGD_2 itself has been shown to exert anti-angiogenic effects in tumors [25], which would pose a second possible principle, so to say macrophage-derived PGD_2 or PGD_2 metabolites diminish the pro-angiogenic effect of other mediators released.

In conclusion of this study, we could show for the first time that HPGDS is upregulated during human monocyte differentiation into macrophages *in vitro*. Additionally, we performed a screening for HPGDS-expressing leukocyte subsets to identify novel potential sources of PGD_2 in pulmonary inflammation. The majority of $CD4^+$ T-cells, NK/T cells, plasma cells and close to all NK cells stained positive for HPGDS, which marks them as potential PGD_2 sources under conditions still to be investigated. Because of a strong link between macrophages and HPGDS expression in ARDS patients, we supposed a central role of macrophages in PGD_2 production in acute lung injury. Although LPS-stimulated MDM released significant amounts of PGD_2, these levels were exceeded tremendously by human monocytes under the same conditions. Due to this finding, a closer look at the role of monocytes in PGD_2 production should be taken into account. Besides looking at PGD_2 production by immune cells, we performed a preliminary experiment investigating the effect of PGD_2-stimulated macrophages on angiogenesis, which is an important factor in pulmonary pathology. PGD_2-stimulation could diminish a pro-angiogenic effect of resting macrophages. Further experiments need to be performed to identify responsible factors, but this effect could be exploited in the future to influence angiogenesis in the lung.

References

1. Aggarwal, N. R., King, L. S. & D'Alessio, F. R. Diverse macrophage populations mediate acute lung inflammation and resolution. *Am J Physiol Lung Cell Mol Physiol* **306,** L709–25 (2014).
2. Fajt, M. L. *et al.* Prostaglandin D2 pathway upregulation: Relation to asthma severity, control, and TH2 inflammation. *J. Allergy Clin. Immunol.* **131,** 1504–1512.e12 (2013).
3. Fujitani, Y. *et al.* Pronounced eosinophilic lung inflammation and Th2 cytokine release in human lipocalin-type prostaglandin D synthase transgenic mice. *J. Immunol.* **168,** 443–9 (2002).
4. Murray, P. J. & Wynn, T. A. Protective and pathogenic functions of macrophage subsets. *Nat. Rev. Immunol.* **11,** 723–737 (2011).
5. Iwasaki, A. & Medzhitov, R. Toll-like receptor control of the adaptive immune responses. *Nat. Immunol.* **5,** 987–995 (2004).
6. Ziegler-Heitbrock, L. *et al.* Nomenclature of monocytes and dendritic cells in blood. *Blood* **116,** e74–80 (2010).
7. Serbina, N. V, Jia, T., Hohl, T. M. & Pamer, E. G. Monocyte-mediated defense against microbial pathogens. *Annu. Rev. Immunol.* **26,** 421–52 (2008).
8. Avraham-Davidi, I. *et al.* On-site education of VEGF-recruited monocytes improves their performance as angiogenic and arteriogenic accessory cells. *J. Exp. Med.* **210,** 2611–25 (2013).
9. Fogg D, Sibon C, Miled C, Jung S,Aucouturier, Dan R. Littman, Ana Cumano, F. G. A clonogenic bone marrow progenitor specific for macrophages and dendritic cells. *Science (80-.).* **311,** 83–88 (2006).
10. Guilliams, M. & van de Laar, L. A Hitchhiker's Guide to Myeloid Cell Subsets: Practical Implementation of a Novel Mononuclear Phagocyte Classification System. *Front. Immunol.* **6,** 406 (2015).
11. Kopf, M., Schneider, C. & Nobs, S. P. The development and function of lung-resident macrophages and dendritic cells. *Nat Immunol* **16,** 36–44 (2015).
12. van Furth, R. & Cohn, Z. A. The origin and kinetics of mononuclear phagocytes. *J. Exp. Med.* **128,** 415–35 (1968).
13. Epelman, S., Lavine, K. J. & Randolph, G. J. Origin and Functions of Tissue Macrophages. *Immunity* **41,** 21–35 (2014).
14. Guilliams, M. *et al.* Alveolar macrophages develop from fetal monocytes that differentiate into long-lived cells in the first week of life via GM-CSF. *J. Exp. Med.* **210,** 1977–92 (2013).

15. Fathi, M. *et al.* Functional and morphological differences between human alveolar and interstitial macrophages. *Exp Mol Pathol* **70,** 77–82 (2001).
16. Cai, Y. *et al.* In vivo characterization of alveolar and interstitial lung macrophages in rhesus macaques: implications for understanding lung disease in humans. *J. Immunol.* **192,** 2821–9 (2014).
17. Duque, G. A. & Descoteaux, A. Macrophage cytokines: Involvement in immunity and infectious diseases. *Front. Immunol.* **5,** 1–12 (2014).
18. Mosser, D. M. The many faces of macrophage activation. *J. Leukoc. Biol.* **73,** 209–212 (2003).
19. Dziarski, R. & Gupta, D. Role of MD-2 in TLR2- and TLR4-mediated recognition of Gram-negative and Gram-positive bacteria and activation of chemokine genes. *J. Endotoxin Res.* **6,** 401–5 (2000).
20. Jaguin, M., Houlbert, N., Fardel, O. & Lecureur, V. Polarization profiles of human M-CSF-generated macrophages and comparison of M1-markers in classically activated macrophages from GM-CSF and M-CSF origin. *Cell. Immunol.* **281,** 51–61 (2013).
21. Gordon, S. Alternative activation of macrophages. *Nat Rev Immunol* **3,** 23–35 (2003).
22. Zhou, D. *et al.* Macrophage polarization and function with emphasis on the evolving roles of coordinated regulation of cellular signaling pathways. *Cell. Signal.* **26,** 192–197 (2014).
23. Varin, A. *et al.* Alternative activation of macrophages by IL-4 impairs phagocytosis of pathogens but potentiates microbial-induced signalling and cytokine secretion. *Blood* **115,** 353–62 (2010).
24. Byers, D. E. & Holtzman, M. J. Alternatively Activated Macrophages and Airway Disease. *Chest* **140,** 768–774 (2011).
25. Lamagna, C., Aurrand-Lions, M. & Imhof, B. a. Dual role of macrophages in tumor growth and angiogenesis. *J. Leukoc. Biol.* **80,** 705–713 (2006).
26. Hanumegowda, C., Farkas, L. & Kolb, M. Angiogenesis in Pulmonary Fibrosis: Too Much or Not Enough? *Chest* **142,** 200–207 (2012).
27. Plafker, S. M. Retinal Degenerative Diseases. *Medicine (Baltimore).* **664,** 447–456 (2010).
28. Sethi, G., Sung, B. & Aggarwal, B. B. TNF: a master switch for inflammation to cancer. *Front. Biosci.* **13,** 5094–107 (2008).
29. Foster, P. S., Rosenberg, H. F., Asquith, K. L. & Kumar, R. K. Targeting eosinophils in asthma. *Curr. Mol. Med.* **8,** 585–90 (2008).
30. Shin, M. H., Lee, Y. A. & Min, D.-Y. Eosinophil-mediated tissue inflammatory responses in helminth infection. *Korean J. Parasitol.* **47 Suppl,** S125–31 (2009).

31. Woerly, G., Roger, N., Loiseau, S. & Capron, M. Expression of Th1 and Th2 immunoregulatory cytokines by human eosinophils. *Int. Arch. Allergy Immunol.* **118,** 95–7
32. Soehnlein, O. & Lindbom, L. Phagocyte partnership during the onset and resolution of inflammation. *Nat. Rev. Immunol.* **10,** 427–439 (2010).
33. San José, E., Sahuquillo, A. G., Bragado, R. & Alarcón, B. Assembly of the TCR/CD3 complex: CD3 epsilon/delta and CD3 epsilon/gamma dimers associate indistinctly with both TCR alpha and TCR beta chains. Evidence for a double TCR heterodimer model. *Eur. J. Immunol.* **28,** 12–21 (1998).
34. LaRosa, D. F. & Orange, J. S. Miniprimer on allergic and immunologic diseases - 1. Lymphocytes. *J. Allergy Clin. Immunol.* **121,** S364–S369 (2008).
35. Spellberg, B. & Edwards, J. E. Type 1/Type 2 immunity in infectious diseases. *Clin. Infect. Dis.* **32,** 76–102 (2001).
36. Kouro, T. & Takatsu, K. IL-5- and eosinophil-mediated inflammation: from discovery to therapy. *Int. Immunol.* **21,** 1303–9 (2009).
37. Walker, J. & Sarmiento, X. Infl ammatory mechanisms in the lung. 1–12 (2009).
38. Lund, F. E. Cytokine-producing B lymphocytes-key regulators of immunity. *Curr. Opin. Immunol.* **20,** 332–8 (2008).
39. Nutt, S. L., Hodgkin, P. D., Tarlinton, D. M. & Corcoran, L. M. The generation of antibody-secreting plasma cells. *Nat. Rev. Immunol.* **15,** 160–171 (2015).
40. Stockley, R. A., Mannino, D. & Barnes, P. J. Burden and Pathogenesis of Chronic Obstructive Pulmonary Disease. *Proc. Am. Thorac. Soc.* **6,** 524–526 (2009).
41. Villar, J., Pérez-Méndez, L. & Kacmarek, R. M. Current definitions of acute lung injury and the acute respiratory distress syndrome do not reflect their true severity and outcome. *Intensive Care Med.* **25,** 930–5 (1999).
42. Gonzales, J. N., Lucas, R. & Verin, A. D. The Acute Respiratory Distress Syndrome: Mechanisms and Perspective Therapeutic Approaches. *Austin J. Vasc. Med.* **2,** (2015).
43. Fanelli, V. *et al.* Acute respiratory distress syndrome: new definition, current and future therapeutic options. *J. Thorac. Dis.* **5,** 326–34 (2013).
44. Grommes, J. & Soehnlein, O. Contribution of neutrophils to acute lung injury. *Mol. Med.* **17,** 293–307 (2011).
45. Beck-Schimmer, B. *et al.* Alveolar macrophages regulate neutrophil recruitment in endotoxin-induced lung injury. *Respir. Res.* **6,** 61 (2005).
46. Jandl, K. *et al.* Activated prostaglandin D2 receptors on macrophages enhance neutrophil recruitment into the lung. *J. Allergy Clin. Immunol.* 1–11 (2016). doi:10.1016/j.jaci.2015.11.012

47. HOLGATE, S. T. Pathogenesis of Asthma. *Clin. Exp. Allergy* **38,** 872–897 (2008).
48. NHI. How is Asthma Treated and Controlled? (2014). Available at: http://www.nhlbi.nih.gov/health/health-topics/topics/asthma/treatment.
49. Lee, J. J. Defining a Link with Asthma in Mice Congenitally Deficient in Eosinophils. *Science (80-.).* **305,** 1773–1776 (2004).
50. Humbles, A. A. A Critical Role for Eosinophils in Allergic Airways Remodeling. *Science (80-.).* **305,** 1776–1779 (2004).
51. Fireman, P. Symposium : Pathophysiology. (2016).
52. Bradding, P., Walls, A. F. & Holgate, S. T. The role of the mast cell in the pathophysiology of asthma. *J. Allergy Clin. Immunol.* **117,** 1277–1284 (2006).
53. Nials, A. T. & Uddin, S. Mouse models of allergic asthma: acute and chronic allergen challenge. *Dis. Model. Mech.* **1,** 213–20 (2008).
54. Chen, H., Bai, C. & Wang, X. The value of the lipopolysaccharide-induced acute lung injury model in respiratory medicine . *Expert Rev Respir Med* **4 ,** 773–783 (2010).
55. Smith, W. L., Urade, Y. & Jakobsson, P. J. Enzymes of the cyclooxygenase pathways of prostanoid biosynthesis. *Chem. Rev.* **111,** 5821–5865 (2011).
56. Qiu, Z. H., de Carvalho, M. S. & Leslie, C. C. Regulation of phospholipase A2 activation by phosphorylation in mouse peritoneal macrophages. *J. Biol. Chem.* **268,** 24506–13 (1993).
57. Dubois, R. N. *et al.* Cyclooxygenase in biology and disease. *FASEB J.* **12,** 1063–1073 (1998).
58. Yoshimura, T., Yoshikawa, M., Otori, N., Haruna, S. & Moriyama, H. Correlation between the Prostaglandin D2/E2 Ratio in Nasal Polyps and the Recalcitrant Pathophysiology of Chronic Rhinosinusitis Associated with Bronchial Asthma. *Allergol. Int.* **57,** 429–436 (2008).
59. Urade, Y. & Eguchi, N. Lipocalin-type and hematopoietic prostaglandin D synthases as a novel example of functional convergence. *Prostaglandins Other Lipid Mediat.* **68-69,** 375–382 (2002).
60. Schuligoi, R. *et al.* PGD2 metabolism in plasma: Kinetics and relationship with bioactivity on DP1 and CRTH2 receptors. *Biochem. Pharmacol.* **74,** 107–117 (2007).
61. Zhao, G. *et al.* Pivotal role of reactive oxygen species in differential regulation of lipopolysaccharide-induced prostaglandins production in macrophages. *Mol. Pharmacol.* **83,** 167–78 (2013).
62. Uchida, Y., Urade, Y., Mori, S. & Kohzuma, T. UV resonance Raman studies on the activation mechanism of human hematopoietic prostaglandin D2 synthase by a divalent cation, Mg2+. *J. Inorg. Biochem.* **104,** 331–340 (2010).
63. Inoue, T. *et al.* Mechanism of metal activation of human hematopoietic prostaglandin

D synthase. *Nat Struct Mol Biol* **10,** 291–296 (2003).

64. Pinzar, E., Miyano, M., Kanaoka, Y., Urade, Y. & Hayaishi, O. Structural basis of hematopoietic prostaglandin D synthase activity elucidated by site-directed mutagenesis. *J. Biol. Chem.* **275,** 31239–31244 (2000).
65. Murata, T. *et al.* Prostagladin D2 is a mast cell-derived antiangiogenic factor in lung carcinoma. *Proc. Natl. Acad. Sci.* **108,** 19802–19807 (2011).
66. Fajt, M. L. *et al.* Prostaglandin D2 pathway upregulation: Relation to asthma severity, control, and TH2 inflammation. *J. Allergy Clin. Immunol.* **131,** 1504–1512.e12 (2013).
67. Murata, T. *et al.* Role of prostaglandin D2 receptor DP as a suppressor of tumor hyperpermeability and angiogenesis in vivo. *Proc. Natl. Acad. Sci. U. S. A.* **105,** 20009–20014 (2008).
68. Ando, M. *et al.* Retrovirally introduced prostaglandin D2 synthase suppresses lung injury induced by bleomycin. *Am. J. Respir. Cell Mol. Biol.* **28,** 582–591 (2003).
69. Urade, Y. & Hayaishi, O. Biochemical, structural, genetic, physiological, and pathophysiological features of lipocalin-type prostaglandin D synthase. *Biochim. Biophys. Acta - Protein Struct. Mol. Enzymol.* **1482,** 259–271 (2000).
70. Narumiya, S., Sugimoto, Y. & Ushikubi, F. Prostanoid receptors: structures, properties, and functions. *Physiol. Rev.* **79,** 1193–226 (1999).
71. Giles, H., Leff, P., Bolofo, M. L., Kelly, M. G. & Robertson, A. D. The classification of prostaglandin DP-receptors in platelets and vasculature using BW A868C, a novel, selective and potent competitive antagonist. *Br. J. Pharmacol.* **96,** 291–300 (1989).
72. Arimura, A. *et al.* Prevention of allergic inflammation by a novel prostaglandin receptor antagonist, S-5751. *J. Pharmacol. Exp. Ther.* **298,** 411–9 (2001).
73. Hirai, H. *et al.* Prostaglandin D2 selectively induces chemotaxis in T helper type 2 cells, eosinophils, and basophils via seven-transmembrane receptor CRTH2. *J. Exp. Med.* **193,** 255–61 (2001).
74. Kostenis, E. & Ulven, T. Emerging roles of DP and CRTH2 in allergic inflammation. doi:10.1016/j.molmed.2006.02.005
75. Stubbs, V. E. L. *et al.* Indomethacin Causes Prostaglandin D2-like and Eotaxin-like Selective Responses in Eosinophils and Basophils. *J. Biol. Chem.* **277,** 26012–26020 (2002).
76. Shichijo, M. *et al.* Chemoattractant receptor-homologous molecule expressed on Th2 cells activation in vivo increases blood leukocyte counts and its blockade abrogates 13,14-dihydro-15-keto-prostaglandin D2-induced eosinophilia in rats. *J. Pharmacol. Exp. Ther.* **307,** 518–25 (2003).
77. Ricciotti, E. & Fitzgerald, G. A. Prostaglandins and inflammation. *Arterioscler.*

Thromb. Vasc. Biol. **31,** 986–1000 (2011).

78. Bradding, P. *et al.* The role of the mast cell in the pathophysiology of asthma. *J. Allergy Clin. Immunol.* **117,** 1277–84 (2006).
79. Murata, T. *et al.* Anti-inflammatory role of PGD2 in acute lung inflammation and therapeutic application of its signal enhancement. *Proc. Natl. Acad. Sci. U. S. A.* **110,** 5205–10 (2013).
80. Sarashina, H. *et al.* Opposing immunomodulatory roles of prostaglandin D2 during the progression of skin inflammation. *J. Immunol.* **192,** 459–65 (2014).
81. Stebbins, K. J. *et al.* Pharmacological blockade of the DP2 receptor inhibits cigarette smoke-induced inflammation, mucus cell metaplasia, and epithelial hyperplasia in the mouse lung. *J. Pharmacol. Exp. Ther.* **332,** 764–75 (2010).
82. Deryugina, E. I. & Quigley, J. P. Chapter 2 Chick Embryo Chorioallantoic Membrane Models to Quantify Angiogenesis Induced by Inflammatory and Tumor Cells or Purified Effector Molecules. *Methods Enzymol.* **444,** 21–41 (2008).
83. McLoughlin, P., Keane, M. P., McLoughlin, P. & Keane, M. P. in *Comprehensive Physiology* (John Wiley & Sons, Inc., 2011). doi:10.1002/cphy.c100034
84. Moghaddami, M., Ranieri, E., James, M., Fletcher, J. & Cleland, L. G. Prostaglandin D(2) in inflammatory arthritis and its relation with synovial fluid dendritic cells. *Mediators Inflamm.* **2013,** 329494 (2013).
85. Endo, Y., Blinova, K., Romantseva, T., Golding, H. & Zaitseva, M. Differences in PGE2 production between primary human monocytes and differentiated macrophages: role of IL-1β and TRIF/IRF3. *PLoS One* **9,** e98517 (2014).
86. Kunz, T., Marklund, N., Hillered, L. & Oliw, E. H. Cyclooxygenase-2, Prostaglandin Synthases, and Prostaglandin H2 Metabolism in Traumatic Brain Injury in the Rat. *J. Neurotrauma* (2004).
87. Tanaka, K. *et al.* Cutting Edge: Differential Production of Prostaglandin D2 by Human Helper T Cell Subsets. *J. Immunol.* **164,** 2277–2280 (2000).
88. Maeno, T. *et al.* CD8+ T Cells Are Required for Inflammation and Destruction in Cigarette Smoke-Induced Emphysema in Mice. *J. Immunol.* **178,** 8090–8096 (2007).
89. Wang, R., Jaw, J. J., Stutzman, N. C., Zou, Z. & Sun, P. D. Natural killer cell-produced IFN-γ and TNF-α induce target cell cytolysis through up-regulation of ICAM-1. *J. Leukoc. Biol.* **91,** 299–309 (2012).
90. Chen, Y., Perussia, B. & Campbell, K. S. Prostaglandin D2 suppresses human NK cell function via signaling through D prostanoid receptor. *J. Immunol.* **179,** 2766–73 (2007).
91. Kim, J. H. *et al.* Natural killer cells regulate eosinophilic inflammation in chronic rhinosinusitis. *Sci. Rep.* **6,** 27615 (2016).

92. Torres, D. *et al.* Prostaglandin D2 inhibits the production of IFN-gamma by invariant NK T cells: consequences in the control of B16 melanoma. *J. Immunol.* **180,** 783–92 (2008).
93. Feng, X. *et al.* Eosinophil production of PGD2 in Aspirin-Exacerbated Respiratory Disease. *J. Allergy Clin. Immunol.* (2016). doi:10.1016/j.jaci.2016.04.042
94. Wright, H. L., Moots, R. J., Bucknall, R. C. & Edwards, S. W. Neutrophil function in inflammation and inflammatory diseases. *Rheumatology (Oxford).* **49,** 1618–31 (2010).
95. LA, K. et. al. The Phyre2 web portal for protein modeling, prediction and analysis. *Nature Protocols 10, 845-858* (2015).